Phase-Field Models

Mathis Plapp
Physique de la Matière Condensée, École Polytechnique, CNRS,
91128 Palaiseau, France

Abstract. Phase-field models have become popular in recent years to describe a host of free-boundary problems in various areas of research. The key point of the phase-field approach is that surfaces and interfaces are implicitly described by continuous scalar fields that take constant values in the bulk phases and vary continuously but steeply across a diffuse front. In the present contribution, a distinction is made between models in which the phase field can be identified with a physical quantity (coarse-grained on a mesoscopic scale), and models in which the phase field can only be interpreted as a smoothed indicator function. Simple diffuse-interface models for the motion of magnetic domain walls, the growth of precipitates in binary alloys, and for solidification are reviewed, and it is pointed out that is such models the free energy function determines both the bulk behavior of the dynamic variable and the properties of the interface. Next, a phenomenological phase-field model for solidification is introduced, and it is shown that with a proper choice of some interpolation functions, surface and bulk properties can be adjusted independently in this model. The link between this phase-field model and the classic free-boundary formulation of solidification is established by the use of matched asymptotic analysis. The results of this analysis can then be exploited to design new phase-field models that cannot be derived by the standard variational procedure from simple free energy functionals within the thermodynamic framework. As examples for applications of this approach, the solidification of alloys and the advected field model for two-phase flow are briefly discussed.

1 Introduction

Phase-field models have rapidly gained popularity over the last two decades in various fields. Some examples for their applications are discussed in recent reviews on the formation of microstructures during solidification by Boettinger et al. (2002) and Plapp (2007), on solid-state transformations

by Chen (2002),Steinbach (2009), and Wang and Li (2010), and on multiphase flows by Anderson et al. (1998), but it is almost impossible to give an exhaustive list of the topics treated with the help of phase-field methods since the development of phase-field models for ever new applications is a rapidly advancing field. All the topics mentioned above have in common that they involve the motion of interfaces or boundaries in response to a coupling of the boundary with one or several transport fields (such as diffusion, flow, stress or temperature fields). This interaction generates morphological instabilities and leads to the spontaneous emergence of complex structures.

All these different models have in common that they describe the geometry of the boundaries through one or several *phase fields*. This name was originally coined in solidification, where the phase field indicates in which thermodynamic phase (solid or liquid) each point of space is located. These fields have fixed pretedermined values in each of the domains occupied by a bulk phase, and vary continuously from one bulk value to the other through an interface that has a well-defined width. In other words, in all phase-field models the interfaces are *diffuse*.

In fact, in the literature, the terms "diffuse-interface model" and "phase-field model" are often used as synonyms. In contrast, in the present contribution I will make a distinction between these two classes of models that is based on the two different and complementary viewpoints that can be taken to derive them. In the first perspective, which could be called "bottom-up", one starts from a microscopic picture of a physical system and performs a *coarse-graining*. While this operation can rarely be carried out explicitly, conceptually it is well defined. As an example, consider a liquid-vapor interface. The relevant quantity that characterizes the difference between the two phases is the number density of molecules, which is high in the liquid but low in the vapor. However, to define a smooth density, the local number of atoms has to be averaged over a volume that is large enough to contain a significant number of molecules, but small enough to remain "local", that is, smaller than any geometric scale of the two-phase pattern to be described. Then, the total free energy of the system may be expressed as a functional that is obtained by averaging all quantities on the coarse-graining scale, and all the coefficients of the functional can in principle be calculated from the elementary intermolecular interactions. The first example for such a model was the van der Waals theory of the liquid-vapor interface, see Rowlinson (1979), but since then many other similar models have been developed, for instance for magnetic domain walls (where the local variable is the magnetization) or interfaces between two phases in a binary mixture (where the relevant variable is the composition). All of these models exhibit diffuse interfaces, whose characteristic thickness agrees with the actual intrinsic

thickness of the physical interfaces, which are indeed microscopically rough and therefore diffuse.

The opposite point of view could be called "top-down". It exploits the scale separation that is inherent to most of the systems mentioned above. Indeed, consider a mixture of two immiscible fluids. The domains occupied by the two fluids can be of any size, but in flows under ordinary conditions droplets are typically of millimetric size. In contrast, the width of the diffuse interfaces between the two fluids is of the order of the molecular size, that is Angstroms for simple fluids and nanometers for polymer mixtures. Therefore, the interface thickness is several orders of magnitude smaller than any geometric length scale of the flow pattern. This is the reason why such problems have been very successfully described as *free boundary problems*: the interfaces are assumed to be mathematically sharp, all quantities that differ between the two phases in contact exhibit jumps at the interfaces, and the transport equations in the bulk phases are solved with explicit boundary conditions imposed at the surface. Capillary forces created by the surface tension are localized at the sharp interfaces and must thus be described by Dirac distributions. This sharp-interface formulation can be perfectly used (and has been used) to perform numerical simulations. However, the handling of the interfaces (which must be discretized in some way) is cumbersome. An obvious idea to make this formulation more amenable to numerical treatment is to smooth out the singularities, that is, to replace step functions and surface delta functions by continuous profiles that have the shape of a smooth kink and a smooth peak, respectively. In this picture, the phase field is just the regularized step (or indicator) function. This regularization of singularities is a mathematically well-defined procedure, which introduces a new length scale into the problem, namely, the typical thickness W of the kink solution, which is *a priori* a free parameter. Quite naturally, the resulting regularized problem will behave differently from the original singular problem. However, the differences disappear in the so-called sharp-interface limit, in which the thickness of the interface tends to zero while all the macroscopic scales remain fixed. A more sophisticated use of this procedure is the so-called thin-interface limit, in which the first-order corrections to the macroscopic problem are calculated and taken into account when choosing the parameters of the phase-field model. In that case, the first corrections to the sharp-interface problem scale as W^2, such that precise simulations can be achieved with much larger values of W. Such models have been termed "quantitative" in the literature; see Karma and Rappel (1996, 1998); Echebarria et al. (2004). Obviously, an upper limit for W is set by the other macroscopic scales present in the problem. Indeed, W must remain much smaller (in practice, about one order

of magnitude) than any geometric length of the two-phase pattern in order that the smoothened version of the problem remains a correct description of the macroscopic geometry.

In the following, I will refer to the models in which the interface is decribed by the profile of a physically accessible quantity as "diffuse-interface models", whereas I will designate by the term "phase-field models" the models in which the interface is described by a smoothed indicator function. While this is not a terminology that is standard in the literature, I believe that it is highly useful to distinghish the two philosophies in order to gain a thorough understanding of the foundations of such models.

For the development of a successful model, it is often advantageous to use both points of view. Indeed, if a new physical situation is considered, it is often quite easy to identify the suitable order parameters together with their symmetries, which gives precious hints for writing down a model that is physically correct. Furthermore, standard out-of-equilibrium thermodynamics then directly gives the equations of motion through a variational procedure. However, models obtained in this way are rarely useful for practical applications, because of the separation of length scales already discussed above. If the diffuse interfaces have the same thickness as the physical ones, the equations need to be discretized on this microscopic scale to correctly resolve the interface profiles. This implies that the length and time scales that can be attained in numerical simulations are severely limited. The only way to access larger system sizes and longer time scales is to use interfaces that are much thicker than the physical ones. However, if the interface thickness is upscaled in a diffuse-interface model, physical effects explicitly linked to the finite interface thickness will generally be amplified, which makes simulation results unreliable. In phase-field models, the separation between the "interface marker" (the phase field) and the directly accessible physical quantities makes it easier to modify the equations in such a way that this amplification of interface effects is avoided.

In the remainder of this article, I will develop several examples which illustrate the relations and distinctions between diffuse-interface and phase-field models, and which demonstrate that phase-field models can be used for obtaining extremely precise results with robust and simple numerical algorithms. In the next section, I will introduce several diffuse-interface models to illustrate some of their properties. In section 3, I will introduce the phase-field model for the solificiation of a pure substance, discuss the difference with diffuse-interface models, and then discuss a method to relate the model parameters to physical quantities for arbitrary interface thickness. Due to space limitations, I will not explicitly display examples the demonstrate the performance of this model, but I will give detailed references to relevant

literature where more details can be found. In section 4, two examples will be given that show how the results of the asymptotic analysis can be used to remove thin-interface effects from phase-field models by adding new terms to the equations that sometimes cannot be derived from free energy functionals within a variational framework. Brief conclusions are given in section 5.

2 Simple diffuse-interface models

In this section, I will introduce some of the simplest diffuse-interface models for subsequent comparison with phase-field models. The presentation will be short and limited to the material that is relevant for the present discussion; more details can be found in the review articles by Hohenberg and Halperin (1977) and Bray (1994), and a particularly pedagogic introduction to some of these models is given by Langer (1991).

2.1 Ising ferromagnet

The Ising model is one of the simplest statistical mechanics models: on a regular lattice, each site is occupied by a microscopic spin variable that can take the values ± 1. Microscopic interactions are between nearest neighbors only, and the interaction favors the alignment of ths spins, that is, two neighboring spins with the same orientation contribute a negative energy. Competition between energy and entropy yields a phase transition at some critical temperature T_c, and for temperatures below T_c, a spontaneous magnetization appears. If a large system is rapidly quenched from above to below T_c, two-phase patterns consisting of "positive" and "negative" domains spontaneously appear. This model has been used as a prototypical example for a system that exhibits domain coarsening, see Bray (1994).

On a mesoscopic level, this system can be decribed by a coarse-grained free energy functional of the Ginzburg-Landau form,

$$F = \int_V \frac{1}{2} K \left(\nabla m\right)^2 + f(m) - hm, \tag{1}$$

where the continuous scalar field $m(\mathbf{x}, t)$ is the local (suitable nondimensionalized) magnetization, obtained by averaging over "coarse-graining" cells of a fixed size ℓ, K is a constant, $f(m)$ is the local free energy density, h is the (dimensionless) external magnetic field (a constant), and the integration is over the entire volume V of the system. The local free energy density $f(m)$ represents the free energy calculated by averaging over all microscopic configurations in a coarse-graining cell for fixed magnetization m. Therefore, its form obviously depends on the size of the coarse-graining cell. From

simple mean-field arguments one obtains that an appropriate form of $f(m)$ is

$$f(m) = \frac{1}{2}a(T - T_c)m^2 + \frac{1}{4}bm^4, \tag{2}$$

where a and b are positive constants, T is the (uniform) temperature, and T_c is the critical temperature of the magnetic phase transition. Note that only even powers of m appear in $f(m)$ because of the up-down symmetry of the magnetic system. For $T < T_c$, $f(m)$ has a double-well structure, and each of the minima correponds to a phase with a spontaneous magnetization. Finally, the gradient square term represents the energy penalty due to magnetization inhomogeneities. The constant K is related to the interaction energy between spins, see for example Langer (1991).

As already mentioned, it is impossible in practice to carry out the coarse-graining procedure; for a recent approximation performed with the help of numerical calculations, see Bronchart et al. (2008). Nevertheless, from a phenomenological point of view, the above functional is reasonable, and the coefficients can be readily adjusted to match a physical system, with the help of four quantities that can in principle be measured: the magnetization, the susceptibility, the magnetic domain wall energy, and the domain wall mobility.

The equilibrium magnetization m^* simply corresponds to the value of m which minimizes $f(m)$ for zero magnetic field ($h = 0$); for the quartic potential given by Eq. (2), it is

$$m^* = \pm\sqrt{\frac{a(T_c - T)}{b}}. \tag{3}$$

Obviously, this minimum is shifted when a magnetic field is applied, since the magnetization tends to align with the external field. The exact value of $m^*(h)$ is the solution of a cubic equation. For small fields, the equation can be linearized around the zero-field solution $m^*(0)$ given by Eq. (3), which yields

$$m^*(h) \approx m^*(0) + \frac{h}{2a(T_c - T)} = m^*(0) + \frac{h}{f''(m^*(0))}, \tag{4}$$

where $f''(m)$ denotes the second derivative of $f(m)$ with respect to m. The magnetic susceptibility $\chi(T)$ is

$$\chi(T) = \left.\frac{dm^*(h)}{dh}\right|_{h=0} = \frac{1}{2a(T_c - T)} = \frac{1}{f''(m^*(0))}. \tag{5}$$

Obviously, the susceptibility diverges when $T \to T_c$, which is one of the signatures of a second-order phase transition.

In order to obtain the magnetic domain wall energy, we first have to determine the profile of the magnetization through a boundary between domains of positive and negative magnetizations. This profile is the minimum of the free energy functional, which can be obtained by evaluating

$$\frac{\delta F}{\delta m} = 0, \tag{6}$$

where the symbol δ denotes the functional derivative. The result of this operation is the equation

$$-K\partial_{xx}m + f'(m) = 0 \tag{7}$$

for a domain wall normal to the x direction, where $f'(m) = df/dm$. This equation has to be solved subject to the boundary condition $m \to m^*(0)$ for $x \to \infty$ and $m \to -m^*(0)$ for $x \to -\infty$. For the quartic potential given by Eq. (2), an explicit solution is available, which is

$$m_0(x) = -m^*(0) \tanh\left(\frac{x - x_0}{\xi}\right), \tag{8}$$

which describes a domain wall centered at the arbitrary position x_0, with

$$\xi = \sqrt{\frac{2K}{a(T_c - T)}} \tag{9}$$

being the characteristic thickness of the domain wall. It can be identified with the correlation length of the magnetization. Note that ξ diverges as $T \to T_c$, as expected for a correlation length in a second-order phase transition.

The quartic potential is widely used in the literature because of the existence of this simple analytic front solution. However, it should be stressed that any double-well potential would produce an equilibrium solution that has a similar structure: a front region in which the variation of m is rapid, surrounded by tails in which m approaches exponentially the minima of the potential.

The fundamental definition of the domain wall energy σ is that σ is the excess free energy due to the presence of a wall. In the absence of an external field h, the two homogeneous solutions $\pm m^*(0)$ have the same free energy. Then, σ can be calculated by the formula

$$\sigma = \frac{F(\text{interface}) - F(\text{homogeneous})}{S}, \tag{10}$$

where $F(\text{interface})$ and $F(\text{homogeneous})$ are the free energies with and without a domain wall, respectively, and S is the surface area along the wall. For a wall normal to the x direction as given by Eq. (8), S cancels out with the integrations along the y and z directions in the free energy functional, such that the above formula simplifies to

$$\sigma = \int_{-\infty}^{\infty} \frac{1}{2} K \left(\partial_x m_0\right)^2 + f(m_0(x)) - f(m^*)\, dx, \tag{11}$$

where we have used that the integrand of Eq. (1) simplifies to $f(m^*)$ for a homogeneous state.

The evaluation of this integral can be greatly simplified by the use of an identity that can be obtained from the equation of the equilibrium profile. Multiplication of both sides of Eq. (7) with $\partial_x m_0$ and integration of the result from $-\infty$ to a certain position x yields (after application of the chain rule)

$$\left[-\frac{K}{2}\left(\partial_x m_0\right)^2\right]_{-\infty}^{x} + \left[f(m_0)\right]_{-\infty}^{x} = 0. \tag{12}$$

Taking into account that $\partial_x m_0$ tends to zero for $x \to \pm\infty$ and that $m_0 \to \pm m^*$ for $x \to \pm\infty$, this simplifies to

$$\frac{K}{2}\left(\partial_x m_0\right)^2 = f(m_0) - f(m^*). \tag{13}$$

This relation is often called "equipartition relation" because it establishes that the two contributions to the free energy excess in Eq. (11) (gradient energy and potential energy) are of equal magnitude. Equation (13) can be used to obtain two important expressions for the surface free energy. In the first, the potential is eliminated, which yields

$$\sigma = \int_{-\infty}^{\infty} K \left(\partial_x m_0\right)^2 \, dx. \tag{14}$$

This expression can be found in many textbooks. The evaluation of this integral requires the knowledge of the equilibrium profile. To circumvent this difficulty, Eq. (13) can also be used to eliminate the gradient energy from Eq. (11), which yields

$$\sigma = \int_{-\infty}^{\infty} 2[f(m) - f(m^*)]\, dx. \tag{15}$$

Furthermore, a simple transformation of Eq. (13) yields

$$\partial_x m_0 = \sqrt{\frac{2[f(m) - f(m^*)]}{K}}. \tag{16}$$

With the help of this relation, it is possible to change the variable of integration from x to m in Eq. (15) and to obtain

$$\sigma = \sqrt{K} \int_{-m^*}^{m^*} \sqrt{2[f(m) - f(m^*)]}\, dm. \tag{17}$$

Therefore, the surface free energy can be calculated from the double-well potential alone, without explicit knowledge of the equilibrium front profile. For the quartic potential of Eq. (2), its value is

$$\sigma = \frac{2\sqrt{2}}{3}\sqrt{K}(m^*)^2\sqrt{a(T_c - T)} = \frac{2\sqrt{2}}{3}\sqrt{K}\frac{[a(T_c - T)]^{3/2}}{b}, \tag{18}$$

where the second identity is obtained with the help of Eq. (3).

Before discussing the front mobility, it is necessary to specify the equation of motion for the magnetization m. In the Ising model, each spin can flip without any constraint. Hence, the local magnetization is a non-conserved quantity. According to non-equilibrium thermodynamics, its rate of change should therefore be proportional to the thermodynamic driving force,

$$\partial_t m = -\Gamma \frac{\delta F}{\delta m}. \tag{19}$$

In other words, the magnetization evolves such as to tend to its local free energy minimum. Here, Γ is a kinetic coefficient which will be taken constant (independent of m and T) for simplicity.

The equilibrium front given by Eq. (8) is stationary. This is natural since the double-well potential is symmetric, and hence the free energy densities of the two phases are identical. Obviously, in the presence of an external magnetic field, this is no longer the case: the phase in which the magnetization is aligned with the external field has a lower free energy and will hence grow at the expense of the other phase by a displacement of the domain wall. For small external fields, the free energy difference of the two phases is simply $\Delta f = 2m^*|h|$. Indeed, the equilibrium values of the magnetization are shifted by the magnetic field according to Eq. (4), but since the free energy curve is symmetric and hence its second derivative is the same in both wells, the shift is the same for both phases and the difference between the equilibrium magnetizations of the two phases remains the same as for zero field (to first order in h). It is to be expected that the velocity of the domain wall is proportional to Δf, the constant of proportionality being the front mobility.

The equation of motion for a steady-state planar front is readily written down in the frame attached to the front, in which $\partial_t = -v\partial_x$:

$$-v\partial_x m = -\Gamma\left[-K\partial_{xx}m + f'(m) - h\right]. \tag{20}$$

For a front which has negative magnetization for $x \to -\infty$, a positive velocity v (corresponding to a migration of the front towards positive x) is obtained for negative magnetic field ($h < 0$) since this favors the growth of the negative domain.

Equation (20) is a nonlinear ordinary differential equation for m. For a given magnetic field h, a solution exists only for specific values of v (for a general discussion of mathematical aspects of front solutions, see van Saarloos (2003)), and a solvability condition then determines v as a function of h. A general analytic solution of this problem is not available for the quartic potential. However, a good approximation can be obtained by the following procedure. Multiply both sides of Eq. (20) with $\partial_x m$ and integrate from $-\infty$ to ∞. The result is

$$v \int_{-\infty}^{\infty} (\partial_x m)^2 = \Gamma \left[-\frac{K}{2} (\partial_x m)^2 + f(m) - hm \right]_{-\infty}^{\infty}. \tag{21}$$

The evaluation of this integral requires the knowledge of the solution $m(x)$ of Eq. (20). However, for small fields it can be supposed that this profile will be close to the equilibrium one (a more detailed justification of this hypothesis will be given below), and the integrals can be evaluated with $m_0(x)$ instead of $m(x)$. With this approximation, since $\partial_x m_0 \to 0$ for $x \to \pm\infty$ and $f(m^*) = f(-m^*)$, the only non-vanishing term on the right hand side arises from the magnetic field, and is equal to $-2m^*h$, the free energy difference. The integral on the left hand side is equal to σ/K according to Eq. (14). Therefore,

$$v \frac{\sigma}{K} = -2\Gamma m^* h = \Gamma \Delta f \tag{22}$$

(recall that h is negative), and the front mobility is simply given by

$$M_{\text{front}} = \frac{\Gamma K}{\sigma}. \tag{23}$$

To summarize, the model has four unknown parameters: the coefficients a and b of the free energy function, the gradient energy coefficient K, and the kinetic constant Γ. They can be uniquely fixed using Eqs. (3), (5), (17), and (23) if the values of four physical quantities are known: the spontaneous equilibrium magnetization m^*, its dependence on the external field (the magnetic susceptibility), the magnetic domain wall energy σ and the front mobility. Note that, since Eq. (2) is a mean-field expression, it does not describe well the free energy density of any real magnetic system, especially close to the critical point. Therefore, the values of a and b that are obtained following the above procedure will certainly depend on the temperature.

Nevertheless, for any fixed temperature this model gives a very satisfactory description of the static and kinetic properties of magnetic domain walls.

It should be noted that the thickness of the domain walls, ξ, is not an independent parameter in this approach, but is given by Eq. (9). Furthermore, the capillary effect is automatically "built in" in this model. This can be easily seen if the above analysis is repeated for a spherical domain of negative magnetization surrounded by an infinite positive domain. Then, in spherical coordinates, the equation for a moving front becomes

$$-v\partial_r m = -\Gamma\left[-K\left(\partial_{rr}m + \frac{d-1}{r}\partial_r m\right) + f'(m) - h\right], \tag{24}$$

where d is the dimension of space. For large domains (of radius $R \gg \xi$), $1/r$ in the second term of the Laplacian can be replaced by $1/R$ since $\partial_r m$ is appreciable only in the interface, which is centered at $r = R$. Then, following the same steps as above yields

$$v\frac{\sigma}{\Gamma K} = -\frac{(d-1)\sigma}{R} - 2m^* h = -\frac{(d-1)\sigma}{R} + \Delta f. \tag{25}$$

For vanishing magnetic field, this identity becomes

$$v = -\Gamma K\frac{(d-1)}{R} = -M_{\text{front}}\sigma\frac{(d-1)}{R}, \tag{26}$$

which describes the so-called *motion by curvature*: the domain wall moves with a velocity that is proportional to its curvature $(d-1)/R$. It can be shown that this equation of motion remains valid even for non-spherical domains; $(d-1)/R$ then has to be replaced by the local mean curvature. Furthermore, local equilibrium ($v = 0$) is achieved if the magnetic field and the curvature are related by

$$2m^* h = -\frac{(d-1)\sigma}{R}. \tag{27}$$

This is called the capillary effect: the equilibrium value of an intensive quantity (here, the magnetic field) is shifted by an amount proportional to the curvature and to the surface free energy.

2.2 Binary lattice gas

Lattice gas models are a convenient setting to describe the thermodynamics and dynamics of two-component systems - be it fluids, polymers or metallic alloys. The systems for which they appear to be the most natural description are binary solid solutions, where the atoms of two different

species occupy the sites of a common crystalline lattice. In the absence of vacancies, a site is occupied either by an A or a B atom. For the simplest case, in which atoms interact only when they occupy nearest neighbor sites, the Hamiltonian of the lattice gas model can be mapped onto the one of the Ising model discussed previously. The energetics (and hence the free energy functional and the thermodynamics that it implies) is hence completely equivalent to the one discussed above. In contrast, the dynamics is completely different: whereas, in the magnetic system, a spin can flip without any constraint, the numbers of A and B atoms are locally and globally conserved quantities, and an A atom cannot "flip" to become a B atom – it can only exchange places with a neighboring B atom.

The quantity that is analogous to the magnetization of the previous subsection is the concentration of one of the species – say, the B atoms. The fraction of B atoms within a coarse-graining cell is denoted by c ($0 \leq c \leq 1$). If the interaction between A and B atoms is weaker than the one between like atoms, *phase separation* will occur below a critical temperature T_c: the thermodynamic equilibrium state is a mixture of two phases, one rich in A and the other rich in B. In anamogy with the Ising model, we can write a free energy functional

$$F = \int_V \frac{K}{2} \left(\nabla c\right)^2 + f(c), \tag{28}$$

with

$$f(c) = \frac{1}{2} a(T - T_c) \left(c - c_c\right)^2 + \frac{b}{4} \left(c - c_c\right)^4 . \tag{29}$$

Here, c_c is the critical concentration at which phase separation first occurs; for a mixture with symmetric interaction constants between the two species, $c_c = 1/2$. Note that there is no term analogous to the external field term in the magnetic free energy functional. The quantity that is analogous to the magnetic field is the conjugate variable of the concentration, which is the chemical potential

$$\mu = \frac{\delta F}{\delta c}. \tag{30}$$

However, contrary to an external magnetic field that can be readily imposed, the application on an "external chemical potential" (for example, by establishing a contact with a "particle reservoir" of fixed properties) is difficult – what is normally imposed is the global concentration. The system then settles down to the thermodynamic equilibrium state, which is characterized by a homogeneous chemical potential.

As already mentioned above, the concentration is a locally conserved quantity. Therefore, is satisfies a continuity equation,

$$\partial_t c = -\nabla \cdot j, \tag{31}$$

where the mass current $\vec{j}$ is driven by the gradient of the chemical potential,

$$j = -M\nabla\mu, \tag{32}$$

with M the atomic mobility (here taken constant for simplicity). Combining these equations and the expression of the free energy yields

$$\partial_t c = M\nabla^2 \frac{\delta F}{\delta c} = M\nabla^2 \left[-K\nabla^2 c + f'(c)\right]. \tag{33}$$

This is called the Cahn-Hilliard equation, after Cahn and Hilliard (1958).

The profile of an equilibrium interface is now determined by the condition of constant chemical potential,

$$\mu = -K\nabla^2 c + f'(c) = \mu_{\mathrm{eq}}, \tag{34}$$

where the value of the equilibrium chemical potential μ_{eq} can depend on the geometry. Bulk thermodynamics tells us that two homogeneous phases (of respective concentrations c_1 and c_2) are in equilibrium if two conditions are fulfilled: the chemical potentials must be equal, that is,

$$\mu_1 = f'(c_1) \equiv \mu_2 = f'(c_2), \tag{35}$$

and the grand potentials $\omega = f - \mu c$ must also be equal,

$$\omega_1 = f(c_1) - \mu_1 c_1 \equiv \omega_2 = f(c_2) - \mu_2 c_2. \tag{36}$$

When expressed graphically, these two equations describe a *common tangent*, a straight line that is tangent to the free energy curve in the two points c_1 and c_2. It is obvious that for the symmetric free energy function given by Eq. (29), the common tangent to the two wells has zero slope ($\mu_{\mathrm{eq}} = 0$). In that case, Eq. (34) becomes identical to Eq. (7). Furthermore, the equilibrium values of the composition simply correspond to the minima of f and are therefore given by the equivalent of Eq. (3):

$$c_1^* = c_c - \sqrt{\frac{a(T_c - T)}{b}} \qquad c_2^* = c_c + \sqrt{\frac{a(T_c - T)}{b}}. \tag{37}$$

However, this is not the only possible equilibrium state. Indeed, consider a spherical domain of the A-rich phase surrounded by an infinite domain

of B-rich phase. Contrary to the spherical magnetic domain treated above, which shrinks according to Eq. (26) unless a magnetic field is applied, the inclusion of A-rich phase cannot evolve since the total number of A atoms (and hence the size of the inclusion) is conserved. The analogy with the magnetic system can nevertheless be exploited: the situation is equivalent to the case where the effects of curvature and magnetic field exactly compensate and the interface is stationary. Indeed, after subtraction of the constant $\mu_{\rm eq}$ on both sides of Eq. (34) and switch to spherical coordinates, it becomes formally identical to Eq. (24) with $v = 0$, with $\mu_{\rm eq}$ being equivalent to h. Hence, the equilibrium chemical potential is given in analogy to Eq. (27) by

$$(c_2 - c_1)\mu_{\rm eq} = -\frac{(d-1)\sigma}{R}, \tag{38}$$

where σ is now the interface free energy, computed as before using the analog of Eq. (17). It should be noted that the *sign* is important here: the chemical potential is *negative* for a spherical inclusion of A-rich phase, whereas it is *positive* for a spherical inclusion of B-rich phase in an A-rich matrix. Formally, this arises from the fact that the integration of c through the interface yields $c_1 - c_2$ on the left-hand side for a B-rich inclusion. Physically, this can be rationalized in the following way. The variable μ is the chemical potential of the B atoms. In the bulk phases (far away from any interface), where the concentration is homogeneous (or at least slowly varying), μ is a function of the local concentration only (the Laplacian in Eq. (30) is negligibly small). Since $f(c)$ is a convex function in the neighborhood of the equilibrium solutions, μ is a monotonously increasing function of c. Therefore, $\mu > 0$ for $c > c_i$ in both phases ($i = 1, 2$). But phase separation takes place because the interactions between like atoms are stronger that between distinct atoms. Since a B atom on the surface of a spherical B-rich inclusion is on average linked by fewer bonds to other B atoms than on a planar interface, its departure into the matrix phase is facilitated, which results in a supersaturation of the matrix phase, that is, $c > c_1$. Of course, the reverse is true for an inclusion of A-rich phase.

The two cases can be easily unified by defining a curvature κ that can be positive and negative. This can be easily done in the following way. In the interfaces, the unit vector

$$\hat{n} = -\frac{\nabla c}{|\nabla c|} \tag{39}$$

is normal to the interfaces and points into the A-rich phase. According to differential geometry, the local curvature of the interface is given by

$$\kappa = \nabla \cdot \hat{n}, \tag{40}$$

which is positive if the B-rich domain is locally convex. With the help of this quantity,

$$\mu_{\rm eq} = \frac{(d-1)\sigma}{c_2 - c_1}\kappa. \tag{41}$$

To complete the picture, we still need the values of c_1 and c_2, which depend of $\mu_{\rm eq}$. For large domains ($R \gg \xi$), where $\mu_{\rm eq}$ is small, we can use a Taylor expansion around $\mu_{\rm eq} = 0$ (where $c_i = c_i^*$) and find

$$\mu_{\rm eq} = 0 + f''(c_i^*)(c_i - c_i^*). \tag{42}$$

For the symmetric double-well potential, the second derivatives are identical, and hence the concentration difference is independent of the curvature and equal to $c_2^* - c_1^*$ (up to first order in the shift). Thus, we find finally

$$c_i = c_i^* + \frac{(d-1)\sigma}{f''(c_i^*)(c_2^* - c_1^*)}\kappa, \tag{43}$$

the so-called Gibbs-Thomson law. Of course, Eq. (42) is completely analogous to Eq. (4), and a generalized susceptibility can be defined by $\chi = 1/f''(c_i^*)$.

The equation of motion for the interfaces is more complicated than for the magnetic model. Because of the conservation law, the motion of an interface is determined by the local flux of B atoms that arrive or depart from the interface. Therefore, no simple local law of motion can be written down, and the calculation of the interface mobility is more involved (see Elder et al. (2001) for a detailed discussion). Nevertheless, the above developments permit to understand a phenomenon of major importance that takes place in alloys, namely, coarsening (Ostwald ripening). Indeed, consider several B-rich inclusions of different sizes in a common A-rich matrix. Since, according to Eq. (42), the chemical potential of B atoms is higher on the surface of smaller inclusions (they have higher cuvature), atoms will diffuse from smaller to larger inclusions. The small inclusions will hence "evaporate" with time. In a finite system, the final equilibrium state is a single spherical inclusion. In an infinite system, the process continues forever and gives rise to a scaling behavior with time that has been much studied, see Bray (1994).

2.3 Second gradient theory for fluids

In the second gradient theory, the dynamics of fluids and of fluid-vapor interfaces is described in terms of the density field ρ, which directly acts as an order parameter to distinguish between the two phases. The model takes

its name from the fact that it can be obtained from a free energy functional that depends not only on the local fluid density, but also on its gradient, in perfect analogy to the models discussed in the previous sections,

$$F = \int_V \frac{1}{2} K \left(\nabla \rho\right)^2 + f(\rho), \tag{44}$$

where $f(\rho)$ is the local free energy density and K is a constant.

Since this model is discussed in great detail for example in Jamet et al. (2001) and also elsewhere in this volume *Roberto: put cross-reference to your contribution if appropriate*, only a few salient facts that are important in the present context will be reviewed. In this case, the free energy function $f(\rho)$ does not have any obvious symmetries, such that on first sight it does not seem appropriate to approach it by a simple symmetric double-well potential. However, if there is liquid-vapor coexistence, the function $f(\rho)$ necessarily has concave parts. Indeed, a thermodynamic chemical potential can be defined by $\tilde{\mu} = \partial f / \partial \rho$, and the conditions for liquid-vapor coexistence are exactly equivalent to those for the binary alloy given above. Therefore, the coexistence densities are obtained by a common tangent construction to the free energy curve. The result of this construction are the coexistence densities as well as the equilibrium chemical potential $\tilde{\mu}_{\rm eq}$. Then, the change of variables $\tilde{\mu} \to \tilde{\mu} - \tilde{\mu}_{\rm eq}$ and $f(\rho) \to f(\rho) - \tilde{\mu}_{\rm eq}\rho$ will transform the free energy density into a double-well potential with minima of equal energy. If a fluid close to its critical point is considered, then this modified free energy density can again be approximated by the symmetric double well potential.

The equation of motion for the fluid density cannot directly be obtained by a variational derivative of F. Instead, ρ satisfies a set of balance equations for mass, momentum, and energy, that has to take into account inertia, viscous dissipation, and the mechanical effect of the surface tension, which creates a capillary force. The resulting equations can be found for example in Jamet et al. (2001). For our discussion, two important points are that the surface tension of this model is given by the analog of Eq. (14),

$$\sigma = \int_{-\infty}^{\infty} K \left(\partial_x \rho_0\right)^2 \, dx, \tag{45}$$

where $\rho_0(x)$ is the density profile across a planar interface normal to the x direction. Of course, this integral can be transformed into one that contains only the free energy density by the same steps as described for the magnetic model in Sec. 2.1. But the free energy function obviously also determines the equations of state of the fluid in the two phases, and thus various thermodynamic quantities such as the isothermal compressibility. In summary,

both the bulk and the surface properties of the model are determined by the choice of the free energy function $f(\rho)$.

2.4 Model C for solidification

The equations of motion for the magnetic model and the alloy model presented above are named "model A" and "model B", respectively, in the review of Hohenberg and Halperin (1977) on dynamic critical phenomena. The idea behind this classification is that in the vicinity of a critical point, static and dynamic properties of many very different systems are universal, and universality classes can be distinguished based on the dimensionality and conservation laws of the involved variables (order parameters). The magnetization is a non-conserved scalar order parameter (model A), the composition is a conserved scalar one (model B). "Model C" in this classification is a model with two scalar fields, one of which is conserved, and the other is non-conserved. The first phase-field models for solidification put forward by Langer (1986), Fix (1983) or Collins and Levine (1985) (see Karma and Rappel (1998) for a brief historic overview of the development of the phase-field model) were just reformulations of this model, with the idea in mind that the non-conserved field corresponds to a structural order parameter (which distinguishes between liquid and solid), whereas the conserved variable represents the diffusion field that limits crystal growth (heat or chemical components).

A starting point for this model is the free energy functional

$$F = \int_V \frac{K}{2} \left(\nabla\phi\right)^2 + H f_{\mathrm{dw}}(\phi) + X u \phi, \tag{46}$$

where ϕ is the phase field, f_{dw} is a dimensionless double-well function – in the following, we will use

$$f_{\mathrm{dw}}(\phi) = \frac{1}{4}(1-\phi^2)^2. \tag{47}$$

Furthermore, K, H, and X are constants, and u is a dimensionless diffusion field (to be defined more precisely below). Since the phase field represents a non-conserved structural order parameter, it obeys the model A dynamics,

$$\partial_t \phi = -\Gamma \frac{\delta F}{\delta \phi}, \tag{48}$$

with the kinetic rate constant Γ. The field u obeys a diffusion equation with a source term,

$$\partial_t u = D\nabla^2 u + \frac{1}{2}\partial_t \phi, \tag{49}$$

where D is a diffusion coefficient.

For the solidification of a pure substance, $u = C(T - T_m)/L$, where T is the local temperature, T_m the melting temperature, and C and L are the specific heat and the latent heat per unit volume, respectively. With this interpretation in mind, it is easy to understand the motivation of the above equations. When $T = T_m$, $u = 0$, and the free energy density of the order parameter is described by a symmetric double-well potential. As a consequence, there is no driving force for solidification since the two phases have the same free energy density. In contrast, for $u \neq 0$, the coupling term $X\phi u$ breaks the symmetry and introduces a free energy difference between the phases. The difference in the free energy density is $\Delta f = 2Xu$ (since the two equilibrium values of ϕ are $\phi^* \approx \pm 1$ and thus their difference is two). Equating this to the free energy difference obtained from standard bulk thermodynamics, $\Delta f = L(T - T_m)/T_m$, and using the definition of u, we can identify

$$X = \frac{L^2}{2CT_m}. \tag{50}$$

This free energy difference induces a motion of the interfaces, since the phase with the lower free energy will form at the expense of the other one. Thus, liquid is transformed into solid (or the reverse), and the latent heat of melting is released (or consumed). This fact is described by the source term in Eq. (49).

A comparison of Eq. (46) to Eq. (1) shows that the free energy functional of model C is identical to the one of the magnetic model, with the free energy density $f(m)$ replaced by $Hf_{\mathrm{dw}}(\phi)$, and the magnetic field h replaced by $-Xu = -Lu/2$. From this, we can immediately deduce that the equilibrium values of ϕ actually depend on the temperature u,

$$\phi^*(u) \approx \pm 1 - \frac{uX}{Hf''_{\mathrm{dw}}(\pm 1)}. \tag{51}$$

Therefore, *ϕ has a non-trivial behavior in the bulk*. As discussed for example by Penrose and Fife (1990), the phase field can indeed be interpreted as a physical quantity (entropy or energy density), such that this model is actually a diffuse-interface model after the classification introduced in Sec. 1. As will be discussed in more detail below, this model is too simple for accurate simulations of crystal growth. But it can still serve as an excellent starting point for the introduction of a more sophisticated model.

3 Solidification of a pure substance

In this section, I will introduce and discuss in some detail the problem of solidification of a pure substance, which has served as one of the standard testing grounds for the development of phase-field modelling. I will start by stating the classic free boundary problem of solidification, and then give the standard phase-field formulation. The differences to the diffuse-interface models described in the previous section will be discussed in some detail. Then, I will describe the method of matched asymptotic expansions that can be used to relate the sharp-interface and phase-field formulations of the solidification problem, and review some salient results obtained with this methodology.

3.1 Sharp-interface formulation

Consider the solidification of a pure substance from its melt. Since the relative change of density upon solidification is small, the density will be assumed to be constant and equal for solid and liquid. Then, no mass transport is needed for crystal growth, which is therefore limited by heat transport, since the latent heat of crystallization that is released upon freezing needs to be evacuated from the growing crystal. Heat transport is assumed to take place by diffusion only; natural convection is neglected. This is a big simplification, which is strictly speaking valid only under microgravity conditions. It is justified by several independent reasons: (i) the purely diffusion-limited case is one of the rare examples where analytical solutions and theories have been developed, and can therefore be studied in its own right, (ii) data from experiments in microgravity are available, see Glicksman et al. (1994), and (iii) this is not a fundamental limitation of the phase-field approach. Indeed, models by Beckermann et al. (1999) or Anderson et al. (2000) that incorporate convection are available, but require much larger computational resources. For the pedagogic exposition intended here, it is thus sufficient to consider the purely diffusive case.

Currents of heat are driven in the liquid and the solid by temperature gradients,

$$j_Q = -k_\nu \nabla T = -C_\nu D_\nu \nabla T, \tag{52}$$

where $\nu = l, s$ labels the two phases, and k_ν is the heat conductivity of phase ν, which is written in the second identity as the product of the specific heat per unit volume C_ν and the thermal diffusion coefficient D_ν. Energy conservation implies that the internal energy density e satisfies

$$\partial_t e = -\nabla \cdot j_Q. \tag{53}$$

We can exploit the definition of the specific heat per unit volume, $C_\nu = de/dT$, to transform this equation for e into one for T. For constant specific heats and constant diffusion coefficients, we obtain simple diffusion equations in both phases,

$$\partial_t T = D_\nu \nabla^2 T. \tag{54}$$

At the interfaces, heat conservation gives rise to a Stefan boundary condition,

$$L v_n = \hat{n} \cdot [j_Q] = \hat{n} \cdot \left[C_s \left. \nabla T \right|_s - C_l \left. \nabla T \right|_l \right], \tag{55}$$

where L is the latent heat of melting per unit volume, v_n is the normal velocity of the interface (counted positive for a growing solid), $\hat{n}$ is the normal vector to the interface pointing into the liquid, and $[j_Q]$ is the difference in heat currents between the two sides of the interface, which is explicitly given in the second identity. The left hand side of this equation represents the heat generated (or absorbed) by a moving interface; this heat is transported by the heat currents in the adjacent material, which are given by the right hand side.

The system of equations is completed with the specification of a boundary condition for the temperature at the interface,

$$T_{\text{int}} = T_m - \frac{\sigma T_m}{L} \kappa - \frac{v_n}{\mu_k}. \tag{56}$$

Here, T_m is the melting temperature, σ the interface free energy, κ the interface curvature, and μ_k the interface mobility. The interface temperature deviates from the bulk thermodynamic equilibrium value T_m by two terms. The first is the capillary shift of the melting temperature (Gibbs-Thomson effect). The second is due to interface kinetics. The fact that μ_k is indeed a mobility can be seen by inverting this equation to obtain v_n, which yields

$$v_n = \mu_k \left[T_{\text{int}} - \left(T_m - \frac{\sigma T_m}{L} \kappa \right) \right]. \tag{57}$$

The interface velocity is hence proportional to the difference of the interface temperature and the curvature-dependent local equilibrium interface temperature, and the proportionality factor is thus a mobility.

It should be noted that the above generalized Gibbs-Thomson law is *isotropic*. In general, the interfacial properties (surface free energy and interface mobility) of a crystal-melt interface are anisotropic (that is, their values depend on the orientation of the surface with respect to the crystallographic axes). While the magnitude of this anisotropy is small for

microscopically rough interfaces (as usually found in metals), its presence is crucial for the selection of dendrite growth directions. Nevertheless, for most of the following we will consider isotropic interfaces for simplicity.

For further simplification, we will consider first the *symmetric model*, in which the diffusion coefficients and the specific heats of solid and liquid are assumed to be identical:

$$C_s = C_l \equiv C \qquad D_s = D_l \equiv D. \tag{58}$$

Then, the above set of equations can be simplified and rewritten in terms of the dimensionless temperature field

$$u = \frac{T - T_m}{L/C}. \tag{59}$$

The result is

$$\partial_t u = D\nabla^2 u \qquad \text{in the bulk,} \tag{60}$$

$$v_n = D\hat{n} \cdot [\nabla u|_s - \nabla u|_l] \qquad \text{at the interface} \tag{61}$$

$$u_{\text{int}} = -d_0\kappa - \beta v_n, \tag{62}$$

where the capillary length d_0 is given by

$$d_0 = \frac{\sigma T_m C}{L^2}, \tag{63}$$

and β is a kinetic coefficient with dimension of inverse velocity,

$$\beta = \frac{C}{\mu_k L}. \tag{64}$$

3.2 Phase-field model

There are several ways to motivate the construction of a suitable phase-field model for this problem. One is to start from bulk thermodynamics. The idea is to introduce a phase field that distinguishes between the two possible phases (solid and liquid). The two values of the phase field that represent solid and liquid can be arbitrarily chosen – we will adopt $\phi = 1$ for the solid and $\phi = -1$ for the liquid. Next, a free energy density needs to be constructed which combines the free energies of the pure phases. For the present case, we may start from the internal energy densities e. Since we have assumed the specific heat $C = de/dT$ to be constant and equal for the two phases, the two curves $e(T)$ are just two parallel straight lines. Furthermore, at the melting temperature T_m, the two free energy densities are equal,

$$f_s = e_s - T_m s_s = f_l = e_l - T_m s_l, \tag{65}$$

with s_s and s_l the entropy densities of the two phases. Furthermore, the definition of the latent heat of melting yields

$$L = e_l(T_m) - e_s(T_m) = T_m(s_l - s_s). \tag{66}$$

Then, up to a constant (which can be omitted) the internal energy density as a function of T and ϕ is

$$e(T, \phi) = C(T - T_m) - \frac{g(\phi)}{2} L, \tag{67}$$

where $g(\phi)$ is an interpolation function that satisfies $g(\pm 1) = \pm 1$. Dividing both sides of this equation by L, we can express the dimensionless internal energy density $\tilde{e} = e/L$ in terms of the dimensionless temperature u introduced above,

$$\tilde{e} = u - \frac{g(\phi)}{2}. \tag{68}$$

The equations of motion of the phase-field model can now be obtained by a variational procedure in the variables $\tilde{e}$ and ϕ from the free energy functional

$$F = \int_V \frac{1}{2} K \left(\nabla \phi\right)^2 + H f_{\mathrm{dw}}(\phi) + \frac{X}{2} \left(\tilde{e} + \frac{g(\phi)}{2}\right)^2 \tag{69}$$

where X is again given by Eq. (50). Indeed, energy is a conserved quantity and hence the internal energy density obeys model B dynamics,

$$\partial_t \tilde{e} = M \nabla^2 \frac{\delta F}{\delta \tilde{e}}, \tag{70}$$

where M is a suitable mobility. In contrast, the phase-field ϕ is a non-conserved variable and thus obeys model A dynamics,

$$\partial_t \phi = -\Gamma \frac{\delta F}{\delta \phi}. \tag{71}$$

Carrying out the functional derivatives, rearranging terms, and using the various definitions introduced previously yields the two equations

$$\partial_t u = D \nabla^2 u + \frac{1}{2} \partial_t g(\phi), \tag{72}$$

$$\Gamma^{-1} \partial_t \phi = K \nabla^2 \phi - H f'_{\mathrm{dw}}(\phi) - \frac{X}{2} g'(\phi) u. \tag{73}$$

For $g(\phi) = \phi$, this is identical to the simple model C presented in Sec. 2.4.

In the following, we will also discuss a slightly more general model, in which Eq. (72) is replaced by

$$\partial_t u = D\nabla^2 u + \frac{1}{2}\partial_t h(\phi), \tag{74}$$

where $h(\phi)$ is a function that satisfies $h(\pm 1) = \pm 1$. This function describes how the latent heat is released through the moving interface and will therefore be called "heat source function". Of course, as soon as $h(\phi) \neq g(\phi)$, the model cannot any longer be obtained by a variational procedure from a free energy functional. However, the equation of motion for ϕ can still be obtained from the functional

$$F' = \int_V \frac{1}{2}K\left(\nabla\phi\right)^2 + Hf_{\rm dw}(\phi) + \frac{X}{2}ug(\phi). \tag{75}$$

In Karma and Rappel (1998), the case $h(\phi) = g(\phi)$ is called the *variational formulation*, whereas the more general case $h(\phi) \neq g(\phi)$ is called the *isothermal variational formulation*.

3.3 Discussion: phase-field vs. diffuse-interface models

The only difference between model C and the phase-field model presented above is the presence of the interpolation function $g(\phi)$ introduced in Eq. (67). The choice of this function has extremely important consequences which merit to be discussed in more detail.

To begin, let us analyze a little further the simple model C. It actually has a major default, which is a consequence of Eq. (51). Indeed, since according to this equation, the equilibrium value of ϕ depends on the temperature, a change of temperature induces a change of the phase field even deep inside the bulk (far away from any interfaces). But this generates sources of latent heat in the bulk according to Eq. (49). This is clearly physically incorrect: latent heat should only be generated or absorbed at moving interfaces according to Eq. (55) of the sharp-interface formulation.

The interpolation function $g(\phi)$ can be used to cure this problem. Repeating the calculations leading to Eq. (51) for the above phase-field model, we find

$$\phi^*(u) \approx \pm 1 - \frac{Xg'(\pm 1)u}{2Hf''_{\rm dw}(m^*(0))}. \tag{76}$$

This, the equilibrium values can be kept *exactly equal* to ± 1 if $g(\phi)$ is chosen such as to have vanishing derivatives at the values of ϕ that correspond to the minima of the double-well potential. For a graphic visualization, the sum $Hf_{\rm dw}(\phi) + (X/2)g(\phi)u$ is plotted in Fig. 1 for suitable values of H,

L and u. The function g actually describes how the double-well potential is *tilted* for $T \neq T_m$. The double-well potential has to be tilted such as to keep the positions of the minima at $\pm$ 1 for arbitrary values of u. For this, the simple linear function $g(\phi) = \phi$ used in model C is not suitable. With the additional requirement that $g(\pm 1) = \pm 1$, the simplest choice is the third-order polynomial

$$g(\phi) = \frac{3}{2}(\phi - \phi^3/3). \tag{77}$$

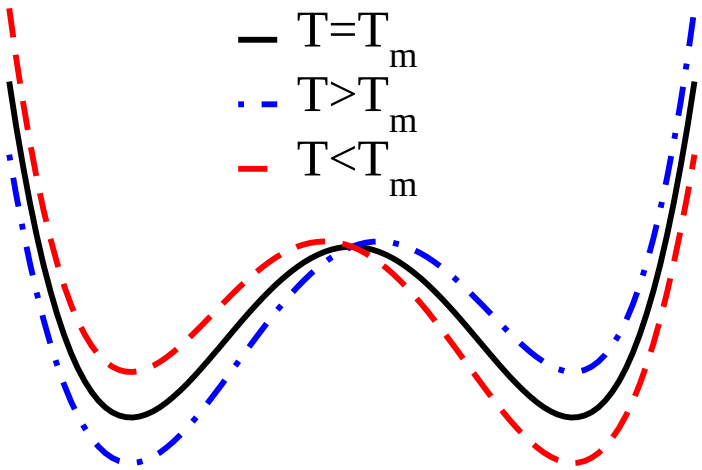

Figure 1. Plot of the tilted double-well potential, with the tilting function $g(\phi)$ given by Eq. (78), for three values of the temperature. The tilt is such that the positions of the minima do not change.

The introduction of the tilting function $g(\phi)$ seems to be only a small change, but it actually has big consequences for the interpretation of the phase field. Since the equilibrium values of ϕ are $\phi^* = \pm 1$ independently of the temperature, it is impossible to identify the phase field with any physically measurable quantity. Indeed, let us first examine the thermodynamic

variables. The phase field exhibits a jump through the interface, just like an extensive quantity. For a pure substance under the assumption of constant density, there are just two such quantities: internal energy density and entropy density. However, the derivatives of both of these quantities with respect to temperature are well-defined quantities: $de/dT = C$, the specific heat per unit volume, as already stated above, and $ds/dT = C/T$ (using the chain rule, $ds/dT = (ds/de)(de/dT)$, and the thermodynamic definition $ds/de = 1/T$). Since $d\phi^*/dT = 0$, the phase field cannot be identified with either of these quantities. Furthermore, the original introduction of the phase field was motivated by the idea of a structural order parameter that distinguishes between solid and liquid. Such an order parameter is either introduced phenomenologically in the spirit of Landau theory, or defined by some microscropic prescription, for example in molecular dynamics simulations, see Hoyt et al. (2003). However, in both cases the equilibrium values of such a quantity also depend on the temperature.

In conclusion, in this model the phase field can only be interpreted as a smoothed indicator field, without direct thermodynamical meaning. It will now be shown that for the purpose of quantitative modeling, this is actually an advantage because is allows to some extent to separate the adjustment of interface and bulk properties. For illustration, let us first calculate the equilibrium front profile. Since equilibrium of a planar front can only occur at $T = T_m$, we have $u = 0$ and the equation of the equilibrium phase field profile becomes

$$K\partial_{xx}\phi - Hf'_{\mathrm{dw}}(\phi) = 0. \tag{79}$$

Dividing both sides of this equation by H, posing

$$W^2 = \frac{K}{H} \tag{80}$$

and carrying out the derivative of f_{dw}, this becomes

$$W^2\partial_{xx} + \phi - \phi^3 = 0, \tag{81}$$

the explicit solution of which is

$$\phi(x) = \tanh\left(\frac{x}{\sqrt{2}W}\right). \tag{82}$$

Therefore, up to a prefactor, W is the front thickness. Repeating the same steps as for the diffuse-interface models, it is easy to obtain the surface tension

$$\sigma = \frac{2\sqrt{2}}{3}\sqrt{KH} = IWH, \tag{83}$$

where $I = 2\sqrt{2}/3$. Qualitatively, this result could have been obtained by a simple dimensional analysis. Indeed, the coefficients K and H in the functional of Eq. (75) have dimensions of energy per unit length and energy per unit volume, respectively. Therefore, the square root of their ratio has dimension of length, and the square root of their product has dimension of energy per unit surface, which is the dimension of a surface free energy. The numerical prefactor I comes from the integration of the double-well potential according to the analog of Eq. (17). Therefore, a different choice for the double-well function will change the interface profile and the value of I, but not the scaling of the physical quantities. The second identity of Eq. (83) has a particularly clear and simple interpretation: the surface free energy scales as the barrier height h in the free energy functional times the front thickness W. Indeed, the parts of the system located in the interface are energetically penalized by an amount of order H and contribute to the surface free energy excess over a thickness W.

Consider now a physical system that has interfaces of a certain physical thickness ξ and surface free energy σ. If, for numerical reasons, we wish to represent this system by a model that has *the same* surface free energy, but a *much larger* interface thickness, $W \gg \xi$, this is easy to achieve in the phase-field model: since σ and W are fixed by the coefficients K and H, it is sufficient to change both at the same time. For example, it is possible to keep σ constant while increasing W by increasing H but desceasing K. At the same time, this change does not affect the thermodynamic behavior of the bulk phases, which is entirely given by the third term in the functional of Eq. (75) that is not affected by changes in K or H.

In contrast, the same operation in model C leads to difficulties. The interfacial properties actually satisfy the same relations as discussed just above, since they do not depend on the presence of the interpolation function $g(\phi)$. But for this model, in addition, the bulk properties of the *physical quantity* that describes the front profile are also determined by the double-well potential according to Eq. (51). For a correct modelling, the variation of ϕ^* with temperature has to be identified with the corresponding thermodynamical quantity, which already fixes the constant H according to Eq. (51). Therefore, a simple rescaling of the double-well potential by the change of H is excluded. It is still possible to modify the surface free energy while keeping the bulk properties constant by more complicated modifications of the double-well potential (keeping the wells unchanged and changing the barrier height, for instance), as tempted for example by Jamet et al. (2001) for a simple diffuse-interface fluid, but the range of the possible modifications is limited.

3.4 Matched asymptotic analysis

Up to now, we have not discussed interface kinetics in the phase-field model. The reason is that its evaluation is considerably more complicated than in the simple models discussed so far. We were able to calculate a simple approximation for the interface mobility in the magnetic model of Sec. 2.1 because the driving force for interface motion was an externally imposed magnetic field, which was homogeneous and constant. In the phase-field model for solidification, the driving force for the phase change is the deviation of the local temperature from the melting temperature. But the temperature field obeys itself a differential equation, is non-homogeneous and time-dependent.

The standard procedure to understand the behavior of a phase-field model and to establish the relation between the model parameters and the physical parameters of the system to be modeled is the method of *matched asymptotic expansions*, a variant of the boundary-layer methods with which the reader might be familiar from fluid dynamics. The basis for these calculations is a *separation of scales* between the front thickness and the other characteristic scales of the problem. Indeed, the problem of solidification can successfully be described by a sharp-interface formulation, in which the interfaces are assimilated to mathematical surfaces without thickness, *because* the physical interfaces have an intrinsic thickness of a few interactomic distances, which is much smaller than any other scale present in the problem.

If this problem is represented by a phase-field model, it is immediately clear that space can be divided in two types of regions. In the bulk phases the phase field is equal to or close to ± 1, the equation of motion for the phase field is trivial, and the temperature field obeys a simple diffusion equation. The bulk phases are separated by a thin but finite layer of *interface*, in which the phase field obeys a non-trivial nonlinear equation that generates source terms in the diffusion equation for the temperature field. Whereas this layer has a complicated overall geometry, the *local* interface properties (curvature, interface velocity) vary only slowly along this layer if scale separation is realized. The central idea of the matched asymptotics is then to solve the non-trivial interface equations in the simple situation where the velocity and the interface curvature are locally constant, and to match this solution to the large-scale solution of the simple diffusion equation away from the interfaces. In this way, the nonlinear interface equations provide *boundary conditions* for the diffusion equation in the bulk.

Technically, the complete calculation is quite cumbersome. It has been presented in detail in several publications, see for example Karma and Rappel (1998), Almgren (1999), or Echebarria et al. (2004). Rather than re-

peating these lengthy developments here, I will restrict the presentation to a simpler problem: the motion of a planar interface with constant velocity. This calculation yields the interface mobility, and illustrates all the steps of the asymptotics. The main physical phenomenon that is missing fron this calculation is the capillary effect. However, its understanding poses no new challenge since it can be calculated at equilibrium, which implies that the temperature field is constant. Therefore, the calculation follows the same lines as for the magnetic model in Sec. 2.1.

It is convenient to make the evolution equations non-dimensional. Let us start by dividing the evolution equation for the phase field, Eq. (73), by the constant H. The result is,

$$\tau\partial_t\phi = W^2\nabla^2\phi - f'_{\rm dw}(\phi) - \lambda g'(\phi)u, \tag{84}$$

where we have defined the phase-field relaxation time $\tau = 1/(\Gamma H)$ and the dimensionless coupling constant

$$\lambda = \frac{X}{2H} = \frac{L^2}{2HCT_m}. \tag{85}$$

This is the standard form of the phase-field equation used in many publications.

Next, we need to choose a "macroscopic" scale for non-dimensionalization of the equations. We follow Almgren (1999) and choose the capillary length d_0, although a different choice yields a simpler calculation for the symmetric model according to Karma and Rappel (1998); however, it is easier to generalize the present calculation to unequal diffusivities. The corresponding time scale is then d_0^2/D. After switching to dimensionless variables, the equations for a planar interface that advances with a constant dimensionless velocity v in the positive x direction are

$$\alpha\epsilon^2\partial_t\phi = -\alpha\epsilon^2 v\partial_x\phi = \epsilon^2\nabla^2\phi - f'_{\rm dw}(\phi) - \lambda u g'(\phi), \tag{86}$$

where $\alpha = D\tau/W^2$, and $\epsilon = W/d_0$ is the scaled interface thickness. The constant λ can actually be eliminated in favor of ϵ. To this end, we invert Eq. (83) to find $H = \sigma/(IW)$, and then eliminate σ by expressing it in terms of the capillary length, Eq. (63). As a result, we obtain

$$\lambda = \frac{I}{2}\frac{W}{d_0} = \frac{I}{2}\epsilon, \tag{87}$$

and the equation for the phase field becomes

$$-\alpha\epsilon^2 v\partial_x\phi = \epsilon^2\nabla^2\phi - f'_{\rm dw}(\phi) - \epsilon I u g'(\phi)/2. \tag{88}$$

The equation for the temperature field in the moving frame is simply

$$\partial_t u = -v\partial_x u = \nabla^2 u + \frac{1}{2}\partial_t h(\phi) = \nabla^2 u - \frac{v}{2}\partial_x h(\phi). \tag{89}$$

The dimensionless interface thickness is in fact the parameter that quantifies the scale separation, since it represents the ratio of the interface thickness W to the "external" physical scales. It is therefore chosen as an expansion parameter in two different expansions in the "outer" and "inner" region,

$$\phi = \hat{\phi}_0 + \epsilon\hat{\phi}_1 + \epsilon^2\hat{\phi}_2 + \ldots \quad \text{outer region} \tag{90}$$

$$\phi = \phi_0 + \epsilon\phi_1 + \epsilon^2\phi_2 + \ldots \quad \text{inner region} \tag{91}$$

$$u = \hat{u}_0 + \epsilon\hat{u}_1 + \epsilon^2\hat{u}_2 + \ldots \quad \text{outer region} \tag{92}$$

$$u = u_0 + \epsilon u_1 + \epsilon^2 u_2 + \ldots \quad \text{inner region.} \tag{93}$$

The outer expansion can be directly inserted in the above equations, and the result is then solved successively order by order. To order zero in ϵ, we obtain from Eq. (88)

$$0 = f'_{\mathrm{dw}}(\hat{\phi}_0), \tag{94}$$

which indicates (as anticipated) that the phase field should assume one of its bulk equilibrium values. Since, thus, $\hat{\phi}_0$ is independent of time, the source term on the right hand side of Eq. (89) is zero, and $\hat{u}_0$ obeys the simple diffusion equation. It is easy to show that these results extend to higher orders in the expansion.

The inner expansion is intended to describe the details of the interface on the scale of the interface thickness W itself. To "zoom in" on this region, we define a *stretched coordinate*

$$\eta = \frac{x}{\epsilon} \tag{95}$$

approprate to this scale. Since, upon the change of variable from x to η, each spatial derivative contributes a factor ϵ^{-1}, the formal effect of this operation is to change the powers of ϵ in each term of the equations. The resulting equations, valid in the inner region, are

$$-\epsilon\alpha v\partial_\eta\phi = \partial_{\eta\eta}\phi - f'_{\mathrm{dw}}(\phi) - \epsilon\frac{I}{2}ug'(\phi), \tag{96}$$

$$-\epsilon^{-1}v\partial_\eta u = \epsilon^{-2}\partial_{\eta\eta}u - \frac{1}{2}\epsilon^{-1}v\partial_\eta\phi. \tag{97}$$

Indeed, comparing Eq. (96) to Eq. (88), it is obvious that the order of the Laplacian term on the right hand side has been changed. This expresses the

fact that the spatial derivatives of ϕ balance the derivative of the double-well potential on the scale of the interface thickness, which precisely leads to a smooth interface.

The explicit calculation of the inner expansion will be given below. Before proceeding, it is useful to state the matching conditions, which are formally defined in the limit when $\epsilon \to 0$,

$$\lim_{\eta \to \pm\infty} \left[u_0(\eta) - \hat{u}_0|^{\pm} \right] = 0, \tag{98}$$

$$\lim_{\eta \to \pm\infty} \left[u_1(\eta) - \hat{u}_1|^{\pm} - \eta \, \partial_x u_0|^{\pm} \right] = 0, \tag{99}$$

where $\hat{u}_n|^{\pm}$ are the limits of the outer fields when the interface is approached from the liquid (+) and the solid (−) side. The conditions for ϕ and for higher order terms of the expansions are similar. The meaning of these formulas is: the asymptotes of the inner fields, extrapolated to the outer region, must match to the local behavior of the outer fields when the interface is approached.

The explicit calculation proceeds as follows. Inserting the expansion for the phase field into Eq. (96) yields at order zero in ϵ

$$0 = \partial_{\eta\eta}\phi_0 - f'_{\mathrm{dw}}(\phi_0), \tag{100}$$

which is just the equation for the equilibrium phase-field profile and has the solution

$$\phi_0 = -\tanh \frac{\eta}{\sqrt{2}} \tag{101}$$

for a solid growing towards positive η. For the temperature field, we find at order ϵ^{-2}

$$0 = \epsilon^{-2} \partial_{\eta\eta} u_0. \tag{102}$$

Taking into account the matching conditions, which imply that $\partial_\eta u_0$ vanishes for $\eta \to \pm\infty$, we can conclude that u_0 is simply a constant, the value of which will be fixed below.

The phase-field equation at order ϵ reads

$$-\alpha v \partial_\eta \phi_0 = \partial_{\eta\eta}\phi_1 - f''_{\mathrm{dw}}(\phi_0)\phi_1 - \frac{I}{2} g'(\phi_0) u_0, \tag{103}$$

where f''_{dw} denotes the second derivative of the double-well function f_{dw}. This is a differential equation for the function ϕ_1. It can be rewritten under the form

$$L_1 \phi_1 = f_1(\eta), \tag{104}$$

with the linear operator $L_1 = \partial_{\eta\eta} - f''_{\rm dw}(\phi_0)$ and the function

$$f_1(\eta) = -\alpha v \partial_\eta \phi_0(\eta) + \frac{I}{2} g'(\phi_0(\eta)) u_0. \tag{105}$$

Since f_1 is a simple function of η, this equation can formally be solved by inverting the linear operator and applying the result to the function on the right hand side. This operation can only be performed if L_1 is invertible. But it is easy to see that L_1 has an eigenfunction with zero eigenvalue, which is $\partial_\eta \phi_0$. Indeed,

$$\left[\partial_{\eta\eta} - f''_{\rm dw}(\phi_0)\right] \partial_\eta \phi_0 = \partial_\eta \left[\partial_{\eta\eta}\phi_0 - f dw'(\phi_0)\right] = 0, \tag{106}$$

and the quantity between square brackets on the right hand side vanishes because it just corresponds to the equilibrium equation for ϕ_0. This mode corresponds in fact to an infinitesimal displacement of the equilibrium front profile, which cannot give a nontrivial now solution. There is therefore a *solvability condition*: the right hand side of Eq. (104) must be orthogonal to this zero-eigenvalue mode, that is,

$$\int_{-\infty}^{\infty} \partial_\eta \phi_0 f_1(\eta) = 0. \tag{107}$$

This condition fixes the value of u_0. Indeed, after plugging in the expression for f_1 and carrying out the integration, we find

$$\alpha v I + I u_0 = 0, \tag{108}$$

(the chain rule yields $\int \partial_\eta \phi_0 g'(\phi_0) = g(-1) - g(1) = -2$), which simplifies to

$$u_0 = -\alpha v. \tag{109}$$

It can be noticed that, since u_0 is just a constant, this result is exactly equivalent to the calculation of the velocity of the magnetic domain wall given by Eq. (22). The procedure of matched asymptotics thus gives a formal justification for the use of the equilibrium profile in the calculation of this velocity, see Eq. (21).

The next order of the diffusion equation reads

$$v \partial_\eta u_0 = \partial_{\eta\eta} u_1 - \frac{v}{2} \partial_\eta h(\phi_0). \tag{110}$$

Since u_0 is a constant, the left hand side vanishes, and the equation can be integrated once to yield

$$\partial_\eta u_1 - \frac{v}{2} h(\phi_0) + A = 0, \tag{111}$$

where A is a constant of integration. This equation immediately yields the Stefan condition. Indeed, comparing the two limiting behaviors for $\eta \to \pm\infty$ we find

$$\lim_{\eta\to-\infty} \partial_\eta u_1 - \lim_{\eta\to\infty} \partial_\eta u_1 = v \tag{112}$$

Furthermore, since we are interested in a steady-state interface, there is no current far inside the solid (that is, $\partial_\eta u_1 \to 0$ for $\eta \to -\infty$), which fixes $A = v/2$ since $h(\phi_0) \to 1$ for $\eta \to -\infty$. Using this result, Eq. (111) can be integrated once more, which yields

$$u_1 = \bar{u}_1 + \frac{v}{2}\int_0^\eta \left[h(\phi_0(\xi)) - 1\right]\, d\xi, \tag{113}$$

where the constant of integration $\bar{u}_1$ can be fixed by the solvability condition for the phase-field equation at the next order,

$$-\alpha v \partial_\eta \phi_1 = \partial_{\eta\eta}\phi_2 + f''_{\mathrm{dw}}(\phi_0)\phi_2 - \frac{I}{2} g'(\phi_0) u_1, \tag{114}$$

which can again be written under the form

$$L_1 \phi_2 = f_2(\eta), \tag{115}$$

where L_1 is the same linear operator as in Eq. (104). In principle, the function ϕ_1 is needed to obtain $f_2(\eta)$. However, simple symmetry arguments show that the contribution of ϕ_1 to the solvability condition vanishes. Indeed, this condition reads

$$\int_{-\infty}^{\infty} \partial_\eta \phi_0 f_2(\eta) = 0. \tag{116}$$

But ϕ_0 is a function that is odd in η ($\phi(-\eta) = -\phi(\eta)$), and thus its derivative is an even function. Therefore, the contribution of any term in f_2 that is odd in η will vanish. Now, ϕ_1 is the solution of Eq. (104) with f_1 given by Eq. (105). Since u_0 is a simple constant, for any function $g(\phi)$ that is odd in ϕ, the right hand side of Eq. (105) is an even function of η. The operator L_1 is also even in η. As a consequence, ϕ_1 must also be even in η, and thus $\partial_\eta \phi_1$ is odd. In fact, several other terms that would be present in a purely formal expansion of the inner phase-field equation have been omitted from Eq. (114) since they do not contribute to the final result due to similar symmetry reasons. In the end, the solvability condition is simply

$$\int \frac{I}{2} g'(\phi_0) u_1(\eta) \partial_\eta \phi_0 \, d\eta = 0, \tag{117}$$

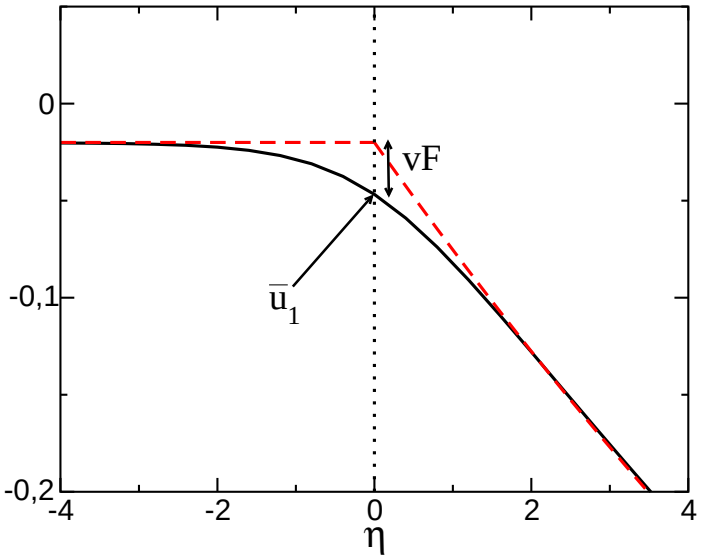

Figure 2. Plot of the temperature field u across a moving planar interface, obtained from a numerical simulation of the model. The dashed lines represent the extrapolations of the asymptotes to the position of the interface, which is indicated by the vertical dotted line. Some of the quantities used in the asymptotic analysis are also indicated: $\bar{u}_1$ is the value of the first-order inner diffusion field at the interface position, and vF is the difference between this value and the "macroscopic" boundary condition.

which yields

$$I\bar{u}_1 = vIJ \tag{118}$$

with J a constant given by

$$J = \int \partial_\eta \phi_0 g'(\phi_0) \left(\int_0^\eta [h(\phi_0(\xi)) - 1] \; d\xi \right) \; d\eta. \tag{119}$$

By this procedure, we have now determined the complete profile of the diffusion field through the interface. However, the boundary condition for the outer field (that is, the value of u that is "seen" on the macroscopic scale) is *not* simply equal to $u_0 + \epsilon\bar{u}_1$. As illustrated in the sketch of Fig. 2, the boundary condition for the outer region is obtained from the application of the matching conditions, Eq. (99), which yields

$$\hat{u}_1|^\pm = \bar{u}_1 + vF^\pm \tag{120}$$

with

$$F^{\pm} = \int_0^{\pm\infty} \left[h(\phi_0) - h(\pm 1) \right] \, d\eta. \tag{121}$$

It is easy to check that for any function $h(\phi)$ odd in ϕ (and in particular for the simplest choice $h(\phi) = \phi$), $F^+ = F^- \equiv F$. This implies that $\hat{u}_1|^+ = \hat{u}_1|^-$, as illustrated in Figure 2. Now we can collect the various pieces of the boundary condition for u, and find

$$u_{\rm int} = \hat{u}_0 + \epsilon \hat{u}_1 = -v \left(\alpha - \epsilon \frac{J + 2F}{4} \right). \tag{122}$$

Switching back to dimensional variables, and inserting the definition of ϵ, the celebrated expression first obtained by Karma and Rappel (1998) for the interface kinetic coefficient is found,

$$\beta = a_1 \frac{\tau}{\lambda W} \left(1 - a_2 \frac{\lambda W^2}{\tau D} \right), \tag{123}$$

with $a_1 = I/2$ and $a_2 = (J + 2F)/(2I)$. Note that our notations slightly differ from those of Karma and Rappel (1998), and that they use a non-normalized version of the tilting function $g(\phi)$, which leads to small differences between the expressions given here and those of Karma and Rappel (1998).

3.5 Rewiev of some results and discussion

Here, some of the essential consequences of the results obtained above will be discussed, and some examples for their application reviewed; for more details, see Karma and Rappel (1998). As already mentioned before, the first term in Eq. (123) is equivalent to the result for domain wall motion under a homogeneous magnetic field. It can be obtained by a simple calculation in which the temperature is assumed to be *constant* in the entire interface, and has been obtained by several authors in the early days of phase-field modeling, see Langer (1986) or Caginalp (1989). The second term in Eq. (123) arises from the fact that the inhomogeneity of the temperature field across the interface is taken into account. In Karma and Rappel (1998), the asymptotics in which the second term is absent is called *sharp-interface limit*, whereas the full procedure is called the *thin-interface limit*. In the calculation presented here, the thin-interface term appears in a higher order of the asymptotic expansion than the sharp-interface term. This could give the impression as if this term would be subdominant in certain conditions. However, this is incorrect: as explicitly demonstrated by

numerical calculations for one-dimensional interfaces in Karma and Rappel (1998), the kinetic behavior of the interface is not correctly described with only the first term in Eq. (123), even in the limit of very slow growth, which corresponds to $\epsilon \to 0$. The physical reason for this behavior is that the heat source term present for moving interfaces has a characteristic scale that is equal to the interface thickness. No matter how small the interface thickness is, there will thus be always a component of the diffusion field that will vary on the scale of the interface. This effect is precisely captured by the above calculation of u_1.

A very important point is that Eq. (123) yields a prescription how to simulate moving interfaces in local equilibrium. This is extremely relevant, since for rough interfaces in metals the interface mobility is large, and thus the kinetic coefficient is small. For the slow growth speeds used in many experiments, kinetic effects can even altogether be neglected, which means that they are adequately described by $\beta = 0$. In the sharp-interface limit, this regime can only be reached when τ tends to zero (which corresponds precisely to a large interface mobility), which leads to equations that are numerically very stiff. The thin-interface expression for β, in contrast, allows for a vanishing kinetic coefficient if W, λ, and τ are related by

$$\tau D = a_2 \lambda W^2. \tag{124}$$

Since $\lambda = a_1 W/d_0$, this is actually a relation between W and τ,

$$\tau = \frac{a_1 a_2}{d_0 D} W^3. \tag{125}$$

Once W is chosen, the above calculation thus fixes the last remaining parameter of the model.

The classic test case for these results is the dendritic growth of a pure substance. To obtain dendrites, anisotropy has to be introduced into the model. Anisotropy of the surface tension can be introduced in the coefficient of the gradient term, or, equivalently, in the interface thickness, whereas an anisotropy in the interface mobility can be introduced in the relaxation time. Both W and τ thus become dependent on the interface orientation,

$$W \to W(\hat{n}) \qquad \tau \to \tau(\hat{n}) \qquad \hat{n} = -\frac{\nabla\phi}{|\nabla\phi|}. \tag{126}$$

Note that the introduction of $W(\hat{n})$ introduces new dependencies on ϕ into the free energy functional and thus generates additional terms in the functional derivative used to obtain the equations of motion, as detailed in Karma and Rappel (1998). These terms implement very naturally the

anisotropic version of the Gibbs-Thomson condition, which is quite complicated when expressed in the sharp-interface model. Dendrites are then simulated by starting from a spherical seed in a uniformly undercooled melt. As long as the interface thickness remains at least about an order of magnitude larger than the tip radius, the growth velocity of the tips at steady state, as well as the entire growth transient, are virtually independent of the interface thickness if τ is chosen accoding to the anisotropic generalization of Eq. (125). It should be mentioned that the phase-field model is currently the method of choice for the simulation of dendritic growth. Old predictions have been confirmed and new interesting phenomena have been discovered, see for example Karma et al. (2000) or Haxhimali et al. (2006). The main advantage with respect to sharp-interface models is the simple and natural treatment of the anisotropic Gibbs-Thomson condition.

Another major result is the comparison between the performances of variational and non-variational models. In the results of the matched asymptotics, the two models differ only by the values of a_1 and a_2. Numerical convergence studies presented in Karma and Rappel (1998) demonstrate that the variational model that uses $h(\phi) = g(\phi)$ with $g(\phi)$ given by Eq. (78) requires a finer grid spacing for convergence than the isothermal variational model with $h(\phi) = \phi$. This can be qualitatively understood from the fact that the heat source function is more strongly peaked in the center of the interface for $h(\phi) = g(\phi)$, and therefore a finer grid spacing is necessary to resolve it with sufficient precision. As a result, the computation times of the non-variational model are about one order of magnitude shorter for comparable numerical precision.

This point merits maybe to be restated in a more pronounced way. Going back to the equations that define the phase-field model, we see from Eq. (68) that the local nondimensionalized internal energy density is given by $\tilde{e} = u + g(\phi)/2$. Whereas, in the variatonal model, the evolution equation for u can be transformed into one for $\tilde{e}$ that takes the form of a conservation law, this is no longer possible for the model with $h(\phi) = \phi$. Thererfore, *heat conservation is violated locally* (on the scale of the interface). Loosely speaking, energy is generated at the front side of the interface and destroyed at the rear. This may seem profoundly shocking. However, since the two local violations of energy conservation exactly compensate, on the macroscopic scale the behavior of the model is in perfect agreement with global energy conservation, and it can therefore safely be used as a computational tool for the resolution of the macroscopic free boundary problem. In conclusion, it may sometimes be advantageous from a computational point of view to disrespect thermodynamics, if this is done in a well-controlled manner, as ascertained by the asymptotic analysis.

4 Phase-field models with additions

In this section, I will discuss two examples for phase-field models that obtain a good performance for the solution of given sharp-interface problems by the addition of supplementary terms in the equations of motion that are justified by the results of asymptotic expansions, and that cannot be obtained by variational derivatives of simple free energy functionals. They are examples for the application of phase-field models outside of the framework of the thermodynamic formalism.

4.1 One-sided solidification and antitrapping current

In the previous chapter, the symmetric model of solidification was discussed in detail. This model is usually a quite good approximation for the solidification of a pure substance, in which the relevant diffusion field is the temperature field. However, a situation of far greater practical importance is the solidification of alloys, in which both heat and chemical components must be exchanged between the growing crystal and its environment. A first remark is that the diffusion of heat is usually much faster than chemical diffusion. Therefore, it is often a good approximation to consider *isothermal solidification*, in which the temperature is supposed to be constant and uniform (in practice, it would be set by a heat bath, which can simply be the bulk of a large ingot, for example). Then, crystal growth is controlled by chemical diffusion only. A second important point is that this chemical diffusion is much faster in the liquid than in the solid (by several orders of magnitude). Therefore, the symmetric model is a very bad approximation for this situation. A much better suited model for this case is the *one-sided model*, in which the diffusion inside the solid is altogether neglected.

Whereas, thus, the natural setting for the one-sided model is alloy solidification, the development of equations of motion that include realistic alloy thermodynamics induces some technical difficulties that are not of interest here. Therefore, we will stick with the model for solidification developed above, and just introduce a diffusion coefficient that depends on the phase field and vanishes in the solid. This corresponds to the two-sided thermal model analyzed also by Almgren (1999). It should be kept in mind that, in the framework of alloy solidification, u represents in fact a non-dimensional chemical potential rather than a temperature.

On first glance, it looks as if the modification of the model is very easy. Introducing a diffusion coefficient of the form

$$D(\phi) = D_l q(\phi), \tag{127}$$

where D_l is the diffusivity in the liquid, and $q(\phi)$ is a dimensionless function

that satisfies $q(-1) = 1$ (liquid) and $q(1) = 0$ (solid), the equations of motion that seem to be appropriate are simply

$$\tau \partial_t \phi = W^2 \nabla^2 \phi - f'_{\mathrm{dw}}(\phi) - \lambda u g'(\phi), \tag{128}$$

$$\partial_t u = D_l \nabla \left(q(\phi) \nabla u \right) + \frac{1}{2} \partial_t h(\phi), \tag{129}$$

where the only difference to the symmetric model is the presence of $q(\phi)$ in the diffusion equation.

However, the asymptotic analysis quickly shows that matters are not so simple. Nothing changes in the first order of the calculation – the "sharp-interface" terms remain the same as for the symmetric model. But a major difference appears at the next order, in the calculation of the second-order diffusion field u_1. Instead of Eq. (113), we find

$$u_1 = \bar{u}_1 + \frac{v}{2} \int_0^\eta \frac{h(\phi_0(\xi)) - 1}{q(\phi_0(\xi)} \, d\xi. \tag{130}$$

Whereas a plot of this diffusion field looks qualitatively similar to the one obtained from Eq. (113), there is an important difference: the two values of the diffusion field, calculated by application of the matching conditions according to Eq. (120), differ from each other, because the two quantities

$$F^{\pm} = \int_0^{\pm\infty} \left[\frac{h(\phi_0) - 1}{q(\phi_0)} - \frac{h(\pm 1) - 1}{q(\pm 1)} \right] \, d\eta. \tag{131}$$

are *not* equal in the one-sided model. As a result, the macroscopic diffusion field exhibits a jump at a moving interface that is proportional to the interface velocity v, the difference $F^+ - F^-$, and to the interface thickness W. The latter point can be appreciated after switching back from dimensionless to dimensional variables in the calculation of u_1. An example of such a jump is shown in Fig. 3. It should be stressed that there is *no discontinuity* in the field u on the scale of the interface – this discuntinuity only appears when the system in seen on the macroscopic scale.

In the framework of alloy solidification, this jump corresponds to the phenomenon of *solute trapping*, which generates indeed a discontinuity of the chemical potential at the interface. It arises from the fact that interface propagation can be much faster than the characteristic speed for exchange of chemical components through the interface. In the classic continuum theory of Aziz (1982), this effect is indeed proportional to both V and W. Therefore, the phase-field model makes a prediction that is qualitatively correct. However, trouble arises if this model is to be used as a computational tool

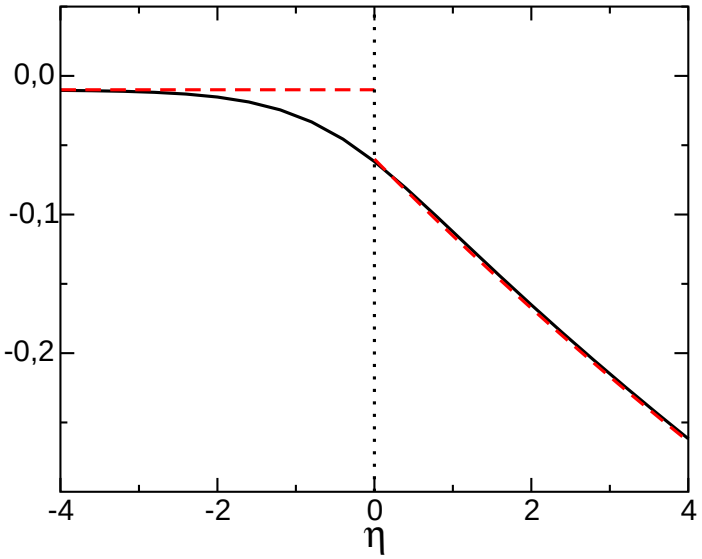

Figure 3. Plot of the temperature field u across a moving planar interface, obtained from a numerical simulation of the one-sided model model. The two extrapolated asymptotes (dashed lines) do not yield the same value of u at the interface (vertical dotted line) on the liquid and the solid side.

in which the interface thickness W is upscaled, because then the magnitude of this effect will be greatly increased, which makes it appreciable even at growth speed where it is completely negligible for the "physical" value of the interface thickness.

In a search how to cure this problem, the one-dimensional calculation performed here cannot give a complete answer. Indeed, an obvious idea is to modify the interpolation functions used in the model to restore the equality $F^+ = F^-$, which makes the solute trapping effect disappear. One possibility to do this that can be deduced from Eq. (131) is to choose $h(\phi)$ in such a way that $(h(\phi) - 1)/q(\phi) = \phi - 1$, which would make the expressions of $F^\pm$ identical to those of the symmetric model with $h(\phi) = \phi$. However, the full two-dimensional calculations carried out in Almgren (1999) and Echebarria et al. (2004) reveal that there are two additional constraints. The reason why these constraints appear only in two dimension is that they imply curvature and diffusion along the interface, respectively. The first concerns the heat source function $h(\phi)$. Consider a curved moving interface. Its length will change with time at a local rate that is given by the product

$v\kappa$. Furthermore, for a curved interface the lengths of the "forward" and "backward" side of the interface are not equal. Therefore, the integration of the heat source term through a moving curved interface gives rise to an excess heat production that is proportional to the interface stretching rate $v\kappa$ and to $H^+ - H^-$, where

$$H^{\pm} = \int_0^{\pm\infty} [h(\phi_0) - h(\pm 1)] \; d\eta. \tag{132}$$

The second correction term concerns diffusion *along* the interface. Indeed, consider a gradient of the diffusion field u along an interface. Since the diffusion coefficient varies through the interface, diffusion will be faster than in the solid on the solid side of the interface, and slower than in the liquid on the liquid side. This will give rise to an additional *surface diffusion* term in the macroscopic equations, unless the two excesses exatcly compensate, that is $Q^+ = Q^-$ with

$$Q^{\pm} = \int_0^{\pm\infty} [q(\phi_0) - q(\pm 1)] \; d\eta. \tag{133}$$

Like the solute trapping effect, both of these additional terms are proportional to the interface thickness. In a quantitatively accurate model, all three need therefore to be eliminated. As already shown in Almgren (1999), it is not possible to achieve this with a reasonable choice of interpolation functions. The new idea put forward by Karma (2001) and further elaborated in Echebarria et al. (2004) is to add a new term, the so-called *antitrapping current* to the diffusion equation in order to counterbalance solute trapping. Since solute trapping acrually corresponds to an engulfment of solute atoms in the advancing interface, this antitrapping current should be directed in the direction normal to the interface and from the solid to the liquid, and be proportional to the interface velocity. Therefore, a reasonable choice is

$$j_{\mathrm{at}} = a(\phi) W \hat{n} \dot{\phi}, \tag{134}$$

where $a(\phi)$ is a new interpolation function, and $\dot{\phi}$ denotes the time derivative of the phase field. With this addition, the diffusion equation for u becomes

$$\partial_t u = D_l \nabla \left(q(\phi) \nabla u \right) - \nabla \cdot j_{\mathrm{at}}. \tag{135}$$

This new ingredient indeed makes it possible to restore the macroscopic continuity of the diffusion field through the interface. Indeed, the calculation of u_1 now yields

$$u_1 = \bar{u}_1 + \frac{v}{2} \int_0^{\eta} p(\phi_0(\xi)) \; d\xi \tag{136}$$

with the function $p(\phi_0)$ given by

$$p(\phi_0) = \frac{h(\phi_0) - 1 - 2a(\phi_0)\partial_\eta \phi_0}{q(\phi_0)}. \tag{137}$$

For the simplest model with $h(\phi) = \phi$ and $q(\phi) = (1-\phi)/2$, the choice of a constant $a(\phi) = 1/(2\sqrt{2})$ yields $p(\phi) = \phi - 1$ and therefore restores a profile of u_1 that is identical to the one of the symmetric model. With this trick, the rest of the asymptotic calculation is unchanged, and the same expression for the kinetic coefficient is obtained than in the symmetric model.

It should be stressed that up to now, no possibility has been found to obtain the antitrapping current from a variational formulation. But it performs very well in numerical calculations, as demonstrated in benchmark simulations in Echebarria et al. (2004). Moreover, up to now no method has been found to formulate a phase-field model that is free from thin-interface effects for an arbitrary ratio of the two diffusivities. As long as the diffusivity in the solid remains much smaller than the one in the liquid, the approach developed for the one-sided model continues to work well. For arbitrary diffusivity ratios, a generalization of the antitrapping current has been developed by Ohno and Matsuura (2009). It works well in situations where the diffusion current on the solid side of the interface remains small. However, as shown by Plapp (2011), in the presence of a non-vanishing current that crosses the interface, a new thin-interface effect appears (interface resistance). So far, it is unclear how this additional effect can be eliminated. In the absence of a solution to this problem, there is no general model for two-phase solidification that has the same efficiency as the ones for the symmetric and the one-sided model.

4.2 The advected field method

The final example for a phase-field model to be discussed is a model for two-phase fluid flow of two immiscible fluids. This is a classic subject in fluid mechanics, and numerous diffuse-interface and phase-field models for this problem have been developed – for a review, see Anderson et al. (1998). Classic approaches are the second gradient method, discussed for example by Jamet et al. (2001), and the convective Cahn-Hilliard equation, see Jacqmin (1999) and elsewhere in the present volume *Roberto: put cross-reference to the part by Anderson.*

An approach that uses the insights from asymptiotic analysis in the spirit of the preceding sections was developed by Folch et al. (1999) for two-phase flow in a Hele-Shaw cell, and later generalized to arbitrary two-phase flows by Biben et al. (2003), who coined the name *advected field method.* The general idea is that for immiscible fluids, there is no mass exchange

across the interface, which is therefore advected by the flow. Furthermore, if the fluids are incompressible, the normal component of the fluid velocity is continous across the interface. Then, the geometry of the fluid domains should be described by a phase-field function that acts as a "marker field", which has no dynamics on its own. This can be achieved with the evolution equation

$$\partial_t \phi + v \cdot \nabla \phi = \Gamma \left[W^2 \left(\nabla^2 \phi - \kappa(\phi) |\nabla \phi| \right) - f'_{\mathrm{dw}}(\phi) \right]. \tag{138}$$

Here, v is an arbitrary velocity field that is the solution of the appropriate fluid flow equation (see below), Γ is a constant, W the interface thickness, and $\kappa(\phi)$ is the local curvature given by

$$\kappa(\phi) = \nabla \cdot \hat{n} = \nabla \cdot \frac{\nabla \phi}{|\nabla \phi|}. \tag{139}$$

The left hand side of Eq. (138) is just the advected derivative of the scalar ϕ. The right hand side without the second term is identical to the expression obtained for the time evolution of m in the magnetic model (model A), see Eq. (20). To understand the role of the additional term, it is useful to analyze what happens to a spherical inclusion of the phase described by $\phi = -1$ inside an infinite matrix of the $\phi = 1$ phase. In this situation, $\nabla \phi = \partial_r \phi$, and $\kappa(\phi)$ is positive according to Eq. (139) since $\partial_r \phi > 0$. Furthermore, the Laplacian written in spherical coordinates is simply $\nabla^2 = \partial_{rr} + ((d-1)/r)\partial_r$. Therefore, Eq. (138) becomes

$$0 = \left[W^2 \left(\partial_{rr} \phi + \frac{d-1}{r} \partial_r \phi - \kappa(\phi) |\nabla \phi| \right) - f'_{\mathrm{dw}}(\phi) \right]. \tag{140}$$

But since $\kappa(\phi) = (d-1)/r$ for any spherically symmetric inclusion, the additional term exactly cancels the $1/r$ term of the Laplacian, such that this equation becomes exactly the equilibrium equation of a planar interface. Thus, the new term $\kappa(\phi)|\nabla \phi|$ is actually a *counterterm* which exactly cancels the driving force for motion by curvature. As a result, the spherical inclusion that would disappear in finite time in the magnetic model is actually an equilibrium configuration here.

This equation was originally developed based on calculations similar to those presented in the previous chapter. Several years later, it was shown by Jamet and Misbah (2008) that, quite surprisingly, this equation can be obtained as the variational derivative of a free energy functional. However, this functional is more complicated than the functionals displayed so far: in addition to the gradient and potential terms present in all the functionals discussed up to now, it contains an additional term that mixes gradients

and the local values of the fields. If this term is chosen in the right way, it guarantees the existence of front solutions *without excess free energy* by creating orbits in the "phase space" of the model (spanned by the values of ϕ and $\nabla\phi$) along which the free energy density is constant and exactly equal to its value at the potential minima. This yields a natural alternative explanation for the properties of this equation: without excess free energy (surface tension), there is indeed no driving force for motion by curvature.

This equation for the phase field has now to be coupled with an equation for fluid flow. As an example, let us take the Navier-Stokes equations for Newtonian fluids,

$$\rho(\phi)\left(\partial_t v + v\cdot\nabla v\right) = \nabla\cdot\sigma_{ij} - \nabla P - \kappa(\phi)\sigma\frac{\nabla\phi}{2}. \tag{141}$$

Here, $\rho(\phi)$ is the phase-dependent density, P is the pressure, σ (without indices) is, as before, the surface tension, whereas $\sigma_{ij} = \eta(\phi)(\partial_i v_j + \partial_j v_i)$ is the Newtonian dissipative stress tensor, with $\eta(\phi)$ the phase-dependent viscosity. The only term which merits further explanations is the last one, which actually represents the capillary force created by the surface tension. Indeed, as usual in phase-field models, this surface force has been transformed into a volumetric force that is "smeared out" over the diffuse interface. For constant curvature κ, an integration of this term through the interface just yields $\kappa\sigma$ since ϕ varies from -1 to 1. Therefore, we recover the Laplace law for the pressure difference between the two sides of a curved interface. The density and the viscosity are interpolated in the usual way, for example for the viscosity we have $\eta(\phi) = \eta_1(1+\phi)/2 + \eta_2(1-\phi)/2$, where η_1 and η_2 are the viscosities of the two fluids.

There are at least two advantages of this approach with respect to the convective Cahn-Hillard equation. First, as discussed in Sec. 2.2, the Cahn-Hilliard equation exhibits Ostwald ripening: when a large and a small droplet are present simultaneously, the small one evaporates and its materials joins the larger one by diffusion. Whereas this is a realistic process, for immiscible fluids the mutual solubilities of the two substances are so low that this process would be extremely slow. The advected field method handles this situation without difficulties: two well-separated drops will remain stationary, whatever are their respective sizes. Second, since the advected field method can be coupled with any fluid flow equation, it is quite easy to extend it to non-Newtonian fluids or even more complex situations. For instance, it has been used for shear-thinning fluids by Nguyen et al. (2010) and for viscoelastic fluids by Beaucourt et al. (2005), as well as (with some modifications) for the time evolution of vesicles by Biben et al. (2005).

5 Summary and Conclusions

In this course, I have presented how phase-field models can be obtained, on the one hand, from the description of the dynamics of first-order phase transitions, and one the other hand from the regularization of macroscopic free-boundary problems. The most important messages can be summarized as follows:

- The models in which interfaces are described as the profile of a physically accessible quantity are easy to obtain from Landau expansions and mean-field arguments, but have numerous computational constraints due to the fact that both the bulk and interface properties of the order parameters are determined by the same free energy curve.
- Phase-field models can alternatively be obtained by starting from the bulk thermodynamics and supplementing it with a dynamical phase field that plays the role of a smoothed indicator function. For a judicious choice of the functions that interpolate the physical quantities between the phases, interface and bulk properties can be chosen independently from each other.
- The link between phase-field models and free-boundary problems can be established quite rigorously by the method of matched asymptotic expansions. As shown for the case of solidification, a correct description of the interface dynamics can only be obtained when *all* phenomena taking place on the scale of the interface thickness are taken into account.
- While it is formally appealing to obtain the equations of motion from a variational formalism, this is not necessary if the goal is to obtain a phase-field formulation for a prescribed free boundary problem. Sometimes, non-variational models may even have large computational advantages.
- Once the asymptotic behavior of a model is well understood, certain properties can be adjusted by adding new terms to the equations of motion.

Only a few simple and fundamental problems that can be solved with phase-field models have been discussed here. The improvement of existing models, and the development of new phase-field models for different physical phenomena is a widely open and very active field of research. An overview over many other applications is given, for example, in the review articles by Emmerich (2008); Steinbach (2009); Wang and Li (2010), and also in several other contributions to the present volume.

Acknowledgments: I thank Tuan Pham Ngoc for a careful proofreading of this manuscript.

Bibliography

R. F. Almgren. Second-order phase field asymptotics for unequal conductivities. *SIAM J. Appl. Math.*, 59:2086–2107, 1999.

D. M. Anderson, G. B. McFadden, and A. A. Wheeler. Diffuse-interface methods in fluid mechanics. *Annual Review of Fluid Mechanics*, 30:139, 1998.

D. M. Anderson, G. B. McFadden, and A. A. Wheeler. A phase-field model of solidification with convection. *PHYSICA D*, 135:175–194, 2000.

M. J. Aziz. Model for the solute redistribution during rapid solidification. *J. Appl. Phys.*, 53(2):1158, 1982.

J. Beaucourt, T. Biben, and C. Verdier. Elongation and burst of axisymmetric viscoelastic droplets: A numerical study. *Phys. Rev. E*, 71:066309, 2005.

C. Beckermann, H.-J. Diepers, I. Steinbach, A. Karma, and X. Tong. Modeling melt convection in phase-field simulations of solidification. *J. Comput. Phys.*, 154:468, 1999.

T. Biben, C. Misbah, A. Leyrat, and C. Verdier. An advected-field approach to the dynamics of fluid interfaces. *Europhys. Lett.*, 63:623, 2003.

T. Biben, K. Kassner, and C. Misbah. Phase-field approach to three-dimensional vesicle dynamics. *Phys. Rev. E*, 72:041921, 2005.

W. J. Boettinger, J. A. Warren, C. Beckermann, and A. Karma. Phase-field simulation of solidification. *Annu. Rev. Mater. Res.*, 32:163–194, 2002.

A. J. Bray. Theory of Phase-ordering kinetics. *Adv. Phys.*, 43:357–459, 1994.

Q. Bronchart, Y. Le Bouar, and A. Finel. New coarse-grained derivation of a phase field model for precipitation. *Phys. Rev. Lett.*, 100:015702, 2008.

G. Caginalp. Stefan and hele-shaw type models as asymptotic limits of the phase-field equations. *Phys. Rev. A*, 39:5887–5896, 1989.

J. W. Cahn and J. E. Hilliard. Free energy of a non-uniform system. 1. interfacial free energy. *J. Chem. Phys.*, 28:258–267, 1958.

L.-Q. Chen. Phase-field models for microstructure evolution. *Annu. Rev. Mater. Res.*, 32:113, 2002.

J. B. Collins and H. Levine. Diffuse interface model of diffusion-limited crystal growth. *Phys. Rev. B*, 31:6119–6122, 1985.

B. Echebarria, R. Folch, A. Karma, and M. Plapp. Quantitative phase-field model of alloy solidification. *Phys. Rev. E*, 70(6):061604, 2004.

K. R. Elder, M. Grant, N. Provatas, and J. M. Kosterlitz. Sharp interface limits of phase-field models. *Phys. Rev. E*, 64:021604, 2001.

H. Emmerich. Advances of and by phase-field modelling in condensed-matter physics. *Adv. Phys.*, 57(1):1–87, 2008.

G. J. Fix. In A. Fasano and M. Primicerio, editors, *Free boundary problems: Theory and applications*, page 580, Boston, 1983. Piman.

R. Folch, J. Casademunt, A. Hernández-Machado, and L. Ramírez Piscina. Phase-field model for hele-shaw flows with arbitrary viscosity contrast. i. theoretical approach. *Phys. Rev. E*, 60(2):1724, 1999.

M. E. Glicksman, M. B. Koss, and E. A. Winsa. Dendritic growth velocities in microgravity. *Phys. Rev. Lett.*, 73:573–576, 1994.

T. Haxhimali, A. Karma, F. Gonzales, and M. Rappaz. Orientation selection in dendritic evolution. *Nature Materials*, 5:660–664, 2006.

P. C. Hohenberg and B. I. Halperin. Theory of dynamic critical phenomena. *Rev. Mod. Phys.*, 49:435–479, 1977.

J. J. Hoyt, M. Asta, and A. Karma. Atomistic and continuum modeling of dendritic solidification. *Mat. Sience Eng. R*, 41:121, 2003.

D. Jacqmin. Calculation of two-phase Navier-Stokes flows using phase-field modeling. *J. Comput. Phys.*, 155:96–127, 1999.

D. Jamet and C. Misbah. Thermodynamically consistent picture of the phase-field model of vesicles: Elimination of the surface tension. *Phys. Rev. E*, 78:041903, 2008.

D. Jamet, O. Lebaigue, N. Coutris, and J. M. Delhaye. The second gradient method for the direct numerical simulation of liquid-vapor flows with phase change. *J. Comput. Phys.*, 169:624–651, 2001.

A. Karma. Phase-field formulation for quantitative modeling of alloy solidification. *Phys. Rev. Lett.*, 87(10):115701, 2001.

A. Karma and W.-J. Rappel. Phase-field method for computationally efficient modeling of solidification with arbitrary interface kinetics. *Phys. Rev. E*, 53(4):R3017–R3020, 1996.

A. Karma and W.-J. Rappel. Quantitative phase-field modeling of dendritic growth in two and three dimensions. *Phys. Rev. E*, 57(4):4323–4349, 1998.

A. Karma, Y. H. Lee, and M. Plapp. Three-dimensional dendrite-tip morphology at low undercooling. *Phys. Rev. E*, 61(4, Part B):3996–4006, APR 2000.

J. S. Langer. An introduction to the kinetics of first-order phase transitions. In C. Godrèche, editor, *Solids far from equilibrium*, Edition Aléa Saclay, pages 297–363, Cambridge, UK, 1991. Cambridge University Press.

J. S. Langer. Models of pattern formation in first-order phase transitions. In G. Grinstein and G. Mazenko, editors, *Directions in Condensed Matter Physics*, pages 165–186, Singapore, 1986. World Scientific.

S. Nguyen, R. Folch, V. K. Verma, H. Henry, and M. Plapp. Phase-field simulations of viscous fingering in shear-thinning fluids. *Phys. Fluids*, 22:103102, 2010.

M. Ohno and K. Matsuura. Quantitative phase-field modeling for dilute alloy solidification involving diffusion in the solid. *Phys. Rev. E*, 79(3): 031603, 2009.

O. Penrose and P. C. Fife. Thermodynamically consistent models of phase-field type for the kinetics of phase transitions. *Physica D*, 43:44–62, 1990.

M. Plapp. Three-dimensional phase-field simulations of directional solidification. *J. Cryst. Growth*, 303:49–57, 2007.

M. Plapp. Remarks on some open problems in phase-field modelling of solidification. *Phil. Mag.*, 91:25–44, 2011.

J. S. Rowlinson. Translation of J. D. van der Waals, The Thermodynamic Theory of Capillarity under the Hypothesis of a Continuous Variation of Density. *J. Stat. Phys.*, 20:197–244, 1979.

I. Steinbach. Phase-field models in materials science. *Model. Simul. Mater. Sci. Eng.*, 17(7):073001, OCT 2009.

W. van Saarloos. Front propagation into unstable states. *Phys. Reports*, 386:29–222, 2003.

Y. Wang and J. Li. Phase field modeling of defects and deformation. *Acta Mater.*, 58:1212–1235, 2010.